

Using community science for detailed pollution research: A case-study approach in Indianapolis, IN, USA

Matthew Dietrich¹, Shelby Rader², and Gabriel Filippelli³

¹Indiana University Purdue University-Indianapolis

²Indiana University

³Indiana University-Purdue University Indianapolis

November 21, 2022

Abstract

Heavy metal contamination in urban environments, particularly lead (Pb) pollution, is a health hazard both to humans and ecological systems. Despite wide recognition of urban metal pollution in many cities, there is still relatively limited research regarding heavy metal distribution and transport at the household-scale between soils and indoor dusts—the most important scale for actual human interaction and exposure. Thus, using community-scientist-generated samples in Indianapolis, IN (United States), we applied bulk chemistry, Pb isotopes, and scanning electron microscopy (SEM) to illustrate how detailed analytical techniques can aid in interpretation of Pb pollution distribution at the household-scale. Our techniques provide definitive evidence for Pb paint sourcing in some homes, while others may be polluted with Pb from past industrial/vehicular sources. SEM revealed anthropogenic particles suggestive of Pb paint and the widespread occurrence of Fe-rich metal anthropogenic spherules across all homes, indicative of pollutant transport processes. The variability of Pb pollution at the household scale evident in just four homes is a testament to the heterogeneity and complexity of urban pollution. Future urban pollution research efforts would do well to utilize these more detailed analytical methods on community sourced samples to gain better insight into where the Pb came from and how it currently exists in the environment. However, these methods should be applied after large-scale pollution screening techniques such as portable X-ray fluorescence (XRF), with more detailed analytical techniques focused on areas where bulk chemistry alone cannot pinpoint dominant pollution mechanisms and where community scientists can also give important metadata to support geochemical interpretations.

38 and mitigating Pb exposure is that its distribution is heterogeneous in urban environments, both
39 at the household and city-wide scale (e.g., Filippelli et al., 2018; Obeng-Gyasi et al., 2021).

40 One approach to better understand Pb heterogeneity in the urban environment is through
41 large sampling datasets at high spatial resolution, collected by community scientists. Community
42 scientists are local community members that can improve scientific research endeavors, bridge
43 the gap between scientists and the general public, enhance the ability to collect samples not
44 easily obtained by researchers alone (i.e., indoor home samples), and provide a link to
45 understanding the critical issues facing communities. While community science thus far has
46 made great strides in improving science communication and mapping Pb exposure risks (e.g.,
47 Filippelli et al., 2018; Ringwald et al., 2021; Watson et al., 2022), there is untapped potential for
48 further research advancement via community science.

49 Although community science samples contain inherent variability with sampling
50 techniques, even with clear instructions, the large sample size of community science endeavors
51 often overcomes this limitation (Filippelli et al., 2018). However, a key question not addressed
52 thus far in community science-based research is whether smaller subsets of samples can be
53 utilized for more detailed geochemical techniques and analyses to understand pollution
54 distributions, despite potential variability in sampling methodology?

55 Lead stable isotopes have frequently been used for tracing pollution sources of Pb in the
56 environment as a more detailed geochemical technique (e.g., Adgate et al., 1998; Jaeger et al.,
57 1998; Sutherland et al., 2003; Wang et al., 2019), largely due to unique Pb isotopic ratios of
58 many Pb sources and minimal environmental and biological fractionation of Pb isotopes (e.g.,
59 Ayuso & Foley, 2020). Despite their applicability in pollution source apportionment studies,
60 complexities arise in urban settings when multiple pollution sources may be present.
61 Additionally, while original Pb ores may oftentimes contain unique Pb isotopic signatures, the
62 diverse range of Pb isotopic ratios in major urban sources such as paint and gasoline can lead to
63 overlap in source ratios (e.g., Resongles et al., 2021; Wang et al., 2021). This can complicate
64 interpretations of Pb pollution sources in environmental media such as soils and dusts, even
65 within a single indoor home, where multiple types of Pb paint, with vastly different isotopic
66 ratios, may persist (Jaeger et al., 1998). Thus, it is often important to not only rely on Pb isotopic
67 ratios when determining pollution sources in the urban environment, but to incorporate other
68 techniques such as bulk chemistry and scanning electron microscopy (SEM) as well. SEM in
69 particular can identify the nature of pollutant particulates (i.e., metal fragments, combustion
70 spherules, etc.) (e.g., Dietrich et al., 2019; Gaberšek & Gosar, 2021), which can help identify the
71 actual form of Pb pollution and thus help differentiate between potential sources when used with
72 other analytical techniques (e.g., Miler & Gosar, 2019).

73 Both SEM and Pb isotope techniques in tandem provide more detailed analytical
74 approaches that can help better parse out Pb pollution sourcing and source distribution compared
75 to bulk chemistry alone. Through four community scientist homes, we provide a case study of
76 how detailed analytical techniques can create a more holistic picture of Pb pollution sourcing and
77 transport in an urban environment. We focus on one typical Midwest US city with known
78 elevated Pb concentrations (Indianapolis, Indiana) as a case study because of the abundance of

79 bulk soil Pb data already collected in the area (Filippelli et al., 2018). We aim to characterize
80 household-scale soil and indoor dust samples to better quantify how Pb sources (i.e., paint and
81 gasoline) are dispersed, and to illustrate how our methodology can be utilized in subsets of large-
82 scale community science projects to address complex patterns uninterpretable based on bulk
83 chemistry alone.

84

85 **2. Materials and Methods**

86 ***2.1 Sampling and Preparation***

87 Soil and dust samples were provided by local community members from four households
88 in Indianapolis (Fig. S1) as part of the Anthropocene Network (<https://anthropocenes.org/lead>),
89 which provides free household screening for Pb (water, dust, and soil sampling) and aims to
90 address issues of environmental equity in the age of the Anthropocene. The community science
91 relationship was enabled through partnerships with local faith leaders in churches and the
92 assurance of participant anonymity, which allowed for sample collection at homes that would
93 otherwise be inaccessible. Residents were instructed to collect bulk vacuum cleaner dust in a
94 sealed plastic bag, as well as soil (upper 0-5 cm) at their home's dripline (directly adjacent to
95 home), the middle of their yard, and directly adjacent to the street with any type of scoop
96 available at their home. Soil samples (~25 g. or more) were placed in separate plastic bags. Each
97 vacuum dust sample was a composite of the entire home, and each soil sample was an individual,
98 non-composite sample. We only selected sampling kits that had clearly labeled sample bags,
99 indicative that the participants followed sampling instructions. Households that were spread out
100 across Indianapolis was also taken into consideration to capture as much potential representation
101 of the city as possible. A small sample size was used because the purpose of this research was to
102 serve as a case study illustrating the ability to utilize community science samples for more
103 detailed analytical research outside bulk soil screening for Pb.

104 All Pb results in the Anthropocene Network were communicated back to anonymous
105 participants with tips on how to mitigate Pb exposure. Because of the emphasis on anonymity,
106 there is sparse metadata for this community science partnership, but other community science
107 endeavors have focused more on participant metadata information (e.g., Dietrich et al., 2022),
108 which can help in interpretation of geochemical results and determining efficient pollutant
109 remediation strategies.

110 Dust samples were sieved at 250 μm and were dry due to the nature of sampling, and thus
111 needed no desiccation. Soil samples were air dried, sieved at 2 mm, then powdered and
112 homogenized utilizing an agate mortar and pestle prior to acid digestion. Samples were weighed
113 (~300-400 mg) into Savillex screw-cap vessels and digested utilizing a multi-stage, three-acid
114 digestion procedure (HF, HNO₃, and HCl), following methods by Rader et al. (2021). Samples
115 were then suspended in 2mL of distilled 8M HNO₃ for column chromatography. A small aliquot
116 of this solution was extracted and diluted for concentration analysis prior to chromatographic
117 separation. This is defined as total soil Pb for the purposes of this study.

118 Samples were purified for Pb isotope analysis via column chromatography utilizing
119 Eichrom Sr Spec resin, slightly modified from that described by Deniel & Pin (2001) and
120 Thibodeau et al. (2007). After purification, samples were diluted accordingly after a
121 concentration check and spiked with NIST 997 thallium (Tl) standard to achieve a Pb/Tl ratio of
122 ~4.

123

124 ***2.2 Instrument Analyses***

125 The metal Pb [along with cadmium (Cd), Tl, and antimony (Sb)—which are reported
126 because of their sparseness in the U.S. urban soil/dust literature] was quantified via an Agilent
127 7700 Inductively Coupled Plasma Mass Spectrometer (ICP-MS), operating in no gas mode. The
128 Pb isotopes ^{204}Pb , ^{206}Pb , ^{207}Pb , and ^{208}Pb were detected with a Nu Plasma II Multicollector
129 Inductively Coupled Plasma Mass Spectrometer (MC-ICP-MS), with the Pb isotope ratios
130 208/206, 207/206, 208/207, 206/204, 207/204, and 208/204 reported after being normalized to
131 Galer & Abouchami (1998). All ICP analyses were completed at Indiana University-
132 Bloomington in the Department of Earth and Atmospheric Sciences' Metal Isotopes Laboratory.
133 More details are provided in Text S1.

134 Dust and soil samples were prepared for SEM and energy dispersive X-ray spectroscopy
135 (EDS) analysis on aluminum samples stubs using carbon sticky tab substrates. EDS lines used to
136 identify Pb specifically include the $L_{\alpha} = 10.541$ keV (nominally $M_{\alpha} = 2.342$ keV, $M_{\beta} = 2.444$
137 keV). All SEM-EDS analyses were conducted at Indiana University-Purdue University
138 Indianapolis, using a Zeiss EVO-10 SEM and Bruker XFlash6, 60 mm² EDS detector.
139 Backscatter electron (BSE) images and EDS data were collected at a setting of 20 kV in variable
140 pressure mode.

141

142 ***2.3 Quality Control***

143 Lead total concentration was deemed acceptable based on a mean recovery of $89.4\% \pm$
144 11.0% ($n = 5$) for NIST SRM 2702 (Table S1) and runs of USGS standard AGV-2a and NIST
145 2702 were both in agreement with previously published Pb isotopic compositions (see Text S2
146 and Table S2). More details on quality control are provided in Text S2.

147

148 **3. Results and Discussion**

149 ***3.1 General Soil and Dust Pb Enrichment and Relationships***

150 Regardless of sample type or location, nearly all samples are enriched relative to the 75th
151 percentile of background soil samples [upper 5 cm of soil, air dried <2 mm fraction crushed to
152 <150 μm prior to a near-total four-acid (hydrochloric, nitric, hydrofluoric, and perchloric)
153 digestion at a temperature between 125 and 150 °C] from throughout Indiana for Pb (Fig. S2;
154 Table S3) (Smith et al., 2013). The 75th percentile value for background soil in Indiana is 25.6

155 mg/kg for Pb. Lead concentrations are ≥ 80 mg/kg in nearly all dust and soil samples (Fig. 1B;
156 Table S3). The general anthropogenic enrichment of Pb (at concentrations in the hundreds to
157 thousands of mg/kg) has been well documented in Indianapolis in urban soils (Filippelli et al.,
158 2018).

159 Although the dust samples were sieved to a finer particle fraction and finer sized particles
160 tend to contain higher concentrations of heavy metals (e.g., Herngren et al., 2006; Tansel &
161 Rafiuddin, 2016), bulk geochemistry results indicate that dust is not consistently higher in metal
162 concentration than the soil samples, even within the same house location (Fig. 1B; Fig. S2). This
163 may indicate that the dominant anthropogenic source for these elements in both media is coarser
164 material, and the interior loading reflects both indoor dust and finer particle invasion from
165 outside. This emphasizes recent work by Gillings et al. (2022) that demonstrates how
166 relationships between indoor and outdoor sources are not always predictable, and inferences on
167 one based on the other should be taken with caution.

168 It is noted that we examined the bulk grain size (<2 mm) composition of outdoor soil
169 samples, and that grain size may affect metal concentrations and partitioning of Pb sources.
170 However, we emphasize that bulk grain size is the most representative way to encapsulate all
171 possible Pb exposure within a household environment. While finer sized particles may be a
172 greater inhalation and transport risk, larger sized particles may degrade over time and still supply
173 a reservoir of Pb pollution.

174

175 **3.2 Bulk Pb Concentration and Pb Isotope Heterogeneity**

176 Three homes displayed clear heterogeneity in bulk metal concentrations of Pb depending
177 on sample location at the home, with only House 1 showing more consistent metal trends for Pb
178 (Fig. 1B; other metals displayed in Fig. S3). This heterogeneity extends to Pb isotopic ratios
179 (Table S4) such as $^{206}\text{Pb}/^{204}\text{Pb}$, although House 2 displayed fairly consistent $^{206}\text{Pb}/^{204}\text{Pb}$ isotopic
180 ratios (Fig. 1A), with slightly more variance in $^{207}\text{Pb}/^{204}\text{Pb}$ and $^{208}\text{Pb}/^{204}\text{Pb}$ ratios (Fig. S4). This
181 matches previous research in urban centers that documented extensive heterogeneity at the
182 household-scale for both bulk metal concentrations such as Pb (e.g., Filippelli et al., 2018;
183 Obeng-Gyasi et al., 2021; Wade et al., 2021) and for Pb isotopic composition (Wang et al.,
184 2021). Due to our small sample size and no consistent trends between Pb isotopes or bulk metal
185 soil concentrations based on sample location, we cannot make any broad generalizations on
186 spatial relationships between dripline, yard, and streetside soils such as larger studies in
187 Indianapolis, IN (Filippelli et al., 2018), Durham, NC (Wade et al., 2021) and Greensboro, NC
188 (Obeng-Gyasi et al., 2021) have done. However, when using bulk Pb concentrations, Pb isotope
189 ratios, and SEM collectively at a house-by-house basis, clearer interpretations of Pb pollution
190 can be made.

191

192 **3.3 Pb Pollution Sources and Pb Distribution by Household—Synthesis of Analytical Methods**

193 *House 1:*

194 The $^{206}\text{Pb}/^{204}\text{Pb}$ isotopic ratio changes significantly depending on the sample location and
195 between the indoor dust and outdoor soil, increasing towards the street, with the dust sample
196 containing the lowest $^{206}\text{Pb}/^{204}\text{Pb}$ isotopic ratio (Fig. 1A). This is not clearly reflected in bulk Pb
197 concentration though, which remains fairly consistent throughout the property, between 70 and
198 130 mg/kg (Fig. 1B; Table S3). Based on Pb isotopes alone, one would interpret a greater
199 proportion of geogenic background glacial till (indicative of surficial Wisconsin glaciation
200 sediments in the area) contribution closer to the street (Fig. S5). However, this is unlikely,
201 because Pb concentrations did not decrease toward the street (Fig. 1B), which would be expected
202 based on much lower Pb concentrations in geogenic background till (Barnes et al., 2020;
203 Kousehlar & Widom, 2020). Thus, the Pb changes in isotopic composition must have come from
204 an additional source of Pb such as leaded paint or leaded gasoline. Microscopy revealed only a
205 few instances of possible Pb paint particles, but routinely revealed evidence of high temperature
206 anthropogenic process Fe-rich spherules at all soil locations (Fig. 2). Thus, while Pb paint likely
207 contributed to bulk Pb inside the home (Fig. 2), the scarcity of distinguishable paint particles via
208 SEM in the soils and prevalence of anthropogenic spherules suggests the possibility of
209 vehicular/industrial Pb sourcing, such as from residual microscopic particulate leaded gasoline or
210 other vehicle Pb-wear (i.e., wheel weights) too small to detect via SEM.

211 *House 2:*

212 There is greater bulk Pb variability in samples than $^{206}\text{Pb}/^{204}\text{Pb}$ ratios on the property
213 (Fig. 1). This includes a dripline soil sample that was 4 mg/kg Pb, and resembled mulching
214 material. Thus, although the house samples are grouped closely on bivariate Pb isotope plots
215 (Fig. S5), Pb sourcing is potentially different between the 4 mg/kg Pb dripline sample and other,
216 more elevated Pb streetside & yard samples. Yard and streetside Pb was much higher than inside
217 the home (Fig. 1B), with SEM imaging revealing no Pb-rich particles inside the home, but
218 several apparent paint Pb-rich particles at the streetside and within the yard, similar to apparent
219 paint particles in Dietrich et al. (2022) (Fig. 2). The prevalence of Pb-rich particles at these
220 locations supports the higher bulk Pb concentrations and suggests that Pb paint abundance
221 outside the home is greater than inside the home, even though Pb isotopic ratios are similar. This
222 may be because of peeling exterior Pb paint that has been reworked in the outdoor environment
223 and covered at the dripline by recent mulch material. There still appears to be an exchange of
224 material across all household samples, as Fe spherules were also found at this household at all
225 locations, even the mulched dripline. However, the spherules at the dripline were less Fe-rich
226 (Fig. S11) than other spherules, suggesting they may have degraded more over time with
227 minerals (i.e., clays, apatite) adhering or precipitating on the spherule structure, or because they
228 were formed under different conditions or processes.

229 *House 3:*

230 Bulk Pb concentrations increase toward the street in soils and are the lowest in dust (Fig.
231 1B; Table S3). $^{206}\text{Pb}/^{204}\text{Pb}$ ratios increase from the dust to the dripline to the yard, but drastically
232 decrease at the streetside (Fig. 1A). SEM did not reveal any Pb paint particles at any location at
233 the home, or any Pb-rich particles of any nature. This suggests reworked, reprecipitated Pb is
234 prevalent in this home environment, likely from historic leaded gasoline because of the increase

235 in Pb concentration towards the street (Fig. 2). Because all samples contain anthropogenic metal
236 spherules, this illustrates the potential for distribution and transport of microscopic aerosol Pb to
237 the home dripline and indoor environment from a distance—either industrial or vehicularly
238 sourced. The widespread dispersion of vehicular Pb from historic leaded gasoline has been
239 observed in atmospheric aerosols in London, U.K. (Resongles et al., 2021), suggesting the
240 potential for the same type of dispersal here. Additionally, the Pb isotopic ratios for streetside
241 soil at this home contain the least ^{206}Pb , ^{207}Pb , and ^{208}Pb relative to ^{204}Pb , which closely aligns
242 with the Pb isotopic range of leaded gasoline (Fig. S5), and House 3 was near a road with the
243 highest modern daily traffic volume compared to any other house in this study (Table S5)—
244 historic traffic volume was likely also high given the urban location.

245 *House 4:*

246 Bulk Pb concentration is highly variable depending on sample location, at the highest (>
247 800 mg/kg) in the dust and dripline soil before decreasing significantly in the yard soil, then
248 increasing in the streetside soil (Fig. 1B). The $^{206}\text{Pb}/^{204}\text{Pb}$ isotopic ratio also changes, increasing
249 from the dust to the dripline soil, then decreasing again for yard and streetside soil (Fig. 1A).
250 Based on microscopy, the dust and dripline soils commonly contain Pb-rich particles resembling
251 paint chips (Fig. 2), and the differences in Pb isotope ratios may be because of different layers or
252 types of paint in the interior versus exterior of the home. Microscopy did not reveal any obvious
253 Pb paint chips in the streetside or yard soils, but did reveal numerous high temperature
254 anthropogenic process Fe-rich spherules, which were evident in both the streetside and dripline
255 soil (Fig. 2). Although there may be mixing of microscopic Pb-rich particles from past vehicular
256 exhaust or other industrial sources at the dripline, that soil is likely more dominated by Pb paint
257 relative to streetside soils, where no Pb paint particles could be easily identified. Thus, because
258 the bulk Pb concentration was still elevated well above background soils (Smith et al., 2013) at
259 the streetside and no Pb paint could be readily identified, residual leaded gasoline, vehicle wear,
260 or other industrial processes was likely the main source of Pb there.

261 **3.3.1 Summary and Comparison of Household Pb Sourcing**

262 The primary Pb sources in all homes were likely Pb-based paint or the remnants of leaded
263 gasoline, supportive of previous literature in urban environments within the U.S. (e.g., Dietrich
264 et al., 2022; Wang et al., 2021). However, each home had different patterns of Pb pollution
265 sources (Table 1) and Pb concentrations (Fig. 1B). This did not seem to be dependent on larger-
266 scale Pb relationships in Indianapolis, such as those at the zip code level (Filippelli et al., 2018).
267 For example, homes 1, 2, and 4 resided in zip codes where reported median Pb concentrations in
268 yard soils ranged from 183-263 mg/kg (Filippelli et al., 2018). However, the Pb concentrations in
269 these homes were widely variable (4-2100 mg/kg; Table S3), and the likely Pb sources changed
270 between paint and vehicular/industrial (i.e., leaded gasoline) both between homes and between
271 sampling location within the homes. Thus, even our small number of households examined in
272 this study exemplifies the fact that generalizations of Pb pollution at larger spatial scales should
273 be made with caution, and multiple other external factors can affect Pb distributions at fine scales
274 such as the history of the home and proximity to major roadways.

275

276 ***3.4 Similarities in Pb Pollution Between Households***

277 Influences on metal concentrations in dusts and soils at the household-scale include not
278 only potential pollution sources, but how dust and soil get reworked and distributed throughout
279 the environment. In general, although there was much Pb pollution heterogeneity between
280 households (Fig. 1), a commonality was the presence of Fe-rich high temperature anthropogenic
281 process spherules at every home within multiple samples (Fig. 2). This entailed homes where
282 distance from road to home was between 7-14 meters, nearby daily traffic volume was highly
283 variable, and where there were multiple possible industrial sources (Table S5). These spherules
284 are commonly seen in industrial urban areas (e.g., Dietrich et al., 2019; Gaberšek & Gosar, 2021)
285 and are likely anthropogenic. This not only suggests that there is exchange of pollutant particles
286 to the dripline of the home, supporting the hypothesis that the side of the home can act as a
287 barrier for particulates to fall following roadside resuspension (e.g., Filippelli et al., 2018;
288 Laidlaw & Filippelli, 2008), but also supports previous studies where there was exchange of
289 outdoor pollution to the indoors (e.g., Adgate et al., 1998; Kelepertzis et al., 2020). Thus,
290 transport of pollutants in soils/dust at the household-scale is likely an additional factor affecting
291 Pb heterogeneity.

292 Future research should therefore consider the ability of metal pollution transport and
293 reworking across neighboring homes and properties. Recent research in other urban settings (i.e.,
294 London) has also pointed out the continued reworking and widespread distribution of historic Pb
295 pollutant particles throughout the environment in the form of atmospheric aerosols (Resongles et
296 al., 2021).

297

298 ***3.5 Limitations of Only Pb Isotopes for Pollution Sourcing***

299 Using Pb isotopes or bulk chemistry alone can be problematic for determining pollutant
300 sourcing, because even within the same home, Pb isotopic composition of paints can vary
301 drastically (Jaeger et al., 1998), and the Pb isotopic ratios for leaded gasoline were widely
302 variable within the U.S. because of changing ore sources over time (e.g., Dietrich et al., 2021).
303 For example, nearly all dust and soil samples plot within 1σ variability of leaded gasoline and
304 lead paint source endmembers depending on the Pb isotope ratios used (Fig. S5). Thus, although
305 previous interpretations in urban settings within the U.S. have concluded Pb paint sources likely
306 dominating soils close to older homes (i.e., built prior to 1978) and leaded gasoline significantly
307 contributing to soils near roadways (e.g., Wade et al., 2021; Wang et al., 2021), we utilized SEM
308 imaging and EDS spectra to aid in interpretation of our variation in bulk Pb and Pb isotopic
309 ratios at the household-scale. This multi-analytical approach is often necessary in complex urban
310 settings where simple binary pollution mixing models of Pb sources will not work—particularly
311 with the increasing overlap of stable Pb isotope signatures of multiple anthropogenic sources
312 (e.g., Resongles et al., 2021).

313

314 4. Implications

315 Urban environments contain complex, heterogenous distributions of heavy metals in soils
316 and dusts, particularly Pb. This is especially evident in a large, post-industrial city such as
317 Indianapolis, IN where historic Pb sources such as leaded paint and leaded gasoline contaminate
318 soils and dusts in varying ways, as shown with differences between our study's household
319 samples. Community science can provide a large sampling set to gather Pb data from, which can
320 effectively help map Pb hotspots, general trends, and inform people of risks in their home (e.g.,
321 Filippelli et al., 2018; Watson et al., 2022). However, there are often nuances associated with
322 pollution interpretations based on bulk chemistry alone, and more detailed analytical methods
323 can help better understand Pb heterogeneity.

324 Here, we demonstrated how detailed methodology such as SEM and Pb isotopes can give
325 a clearer picture of Pb pollution source distribution on a property. This approach can be utilized
326 for even larger subsets of community science samples to better understand pollution variability
327 in bulk chemistry following initial screening through techniques such as X-ray fluorescence
328 (XRF). While there is inherent uncertainty in sampling with community scientists, as long as
329 general instructions are followed, enough information may be gathered to obtain informative
330 and actionable insight into pollution sources distributions. For example, whether Pb pollution
331 from the home reaches the street, or whether Pb pollution from the street reaches the home. This
332 information can therefore aid in home pollution remediation and prevention by determining
333 whether there is significant transport and exchange of Pb pollution sources.

334 Additionally, working more with community members as real partners in research can be
335 helpful for both gaining useful information to interpret Pb pollution results and helping the
336 community members to place these results in their household context. This is a different
337 approach that “parachute science” and has more lasting effects in changing behavior (Hayhow et
338 al., 2021). For example, we recommend surveying community members first about their
339 concerns and gathering important metadata during the course of the study, such as the age of
340 their home, whether there has been recent renovation, worries of a particular Pb source nearby,
341 etc.

342 Future studies in urban centers throughout the world would do well to capitalize on
343 community science and the multi-analytical techniques such as those used here and in other
344 recent urban metal pollution studies (e.g., Gaberšek & Gosar, 2021; Kelepertzis et al., 2021) to
345 more fully understand the nuance associated with urban metal pollution distributions. This can be
346 important in determining whether a pollutant source is coming from a property or elsewhere, the
347 nature of the pollutant particles (i.e., are there Pb particles that are small enough to be an
348 inhalation risk), and whether there is transfer of material from inside to outside a home. All these
349 details are helpful from both a health risk and remediation perspective.

350 These techniques should be particularly used more within the U.S. because of the
351 abundance of urban centers with varying legacies of pollution, the demographic and climate
352 diversity, and the growing popularity of community science research providing an abundance of
353 samples to study (e.g., Filippelli et al., 2018; Ringwald et al., 2021). These community science

354 endeavors offer a cost-effective way to systematically choose subsets of samples for more
355 detailed multi-analytical approaches that provide important and scalable insight into Pb
356 pollution. Lastly, these community science efforts expand the possible options for sample
357 accessibility to researchers, such as to household indoor dust samples.

358

359 **Acknowledgements**

360 The authors are deeply thankful to the households that supplied samples for this work and
361 the lab techs who helped with initial sampling processing. The Anthropocene Network is
362 supported by the Environmental Resilience Institute, funded by Indiana University's Prepared for
363 Environmental Change Grand Challenge Initiative. Partial support for this work was provided by
364 NSF-EAR-PF Award #2052589 to M.D. Special thanks to Miguel Cruz for help with SEM
365 instrumentation, Jason Kelly with help providing the samples, the two anonymous reviewers for
366 their insightful comments, and Leah Wood and John Shukle for helpful comments on an earlier
367 version of the manuscript.

368

369 **Manuscript Tables:**

370

371 **Table 1:** Summary of the likely primary Pb pollution sources by house and sampling location.

House	Indoor Dust	Dripline	Yard	Streetside
1	Paint	Vehicular or industrial	Vehicular or industrial	Vehicular or industrial
2	Potentially Paint	None	Paint	Paint
3	Vehicular or industrial	Vehicular or industrial	Vehicular or industrial	Vehicular or industrial
4	Paint	Paint	Potentially Paint/Vehicular	Vehicular or industrial

372

373

374

375

376

377

378

379

380

381 **Manuscript Figures:**

382

383

384

385

386

387

388

389

390

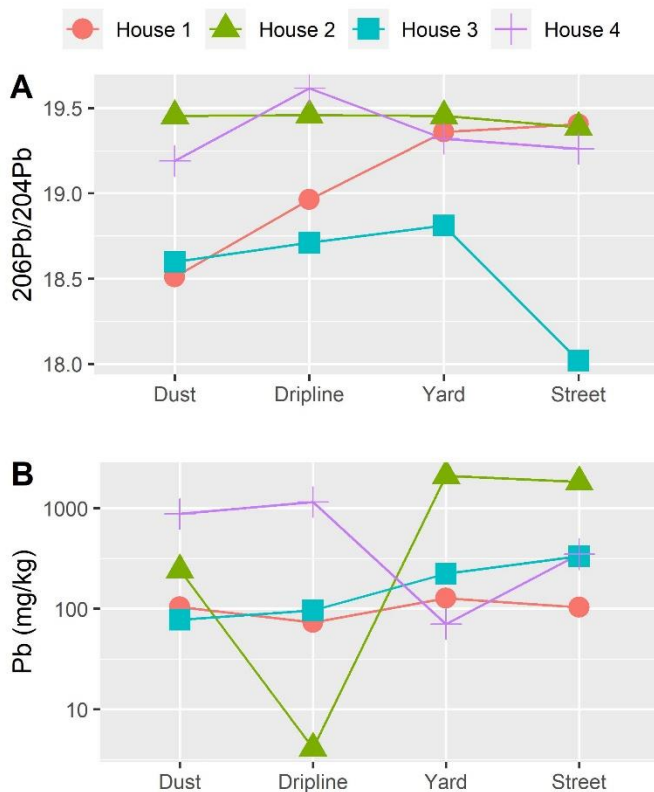
391

392

393

394

395



396 **Fig. 1:** Trends in $^{206}\text{Pb}/^{204}\text{Pb}$ based on sample type and house (A), as well as trends in bulk Pb
397 concentration (mg/kg) based on sample type and house (B). Similar trends were seen for other
398 isotopic ratios, albeit with slight variability (Fig. S4).

400 **Fig. 2:** Bivariate plot of Pb isotopic ratios, grouped by house and sample location. 2σ analytical
401 variability is minimal relative to the sample symbol size and are thus only displayed in Table S2.
402 SEM images are listed below the plot, with anthropogenic particles outlined in white. The
403 corresponding EDS spectra for each superscript notation are listed in the Supplementary
404 Information (Figs. S6-S21). Images labeled “Pb” contain Pb-rich particles within the white
405 outline, while images labeled “Fe” contain Fe-rich particles within the white outline. It is noted
406 that the paint particles in House 2: Streetside⁷, House 4: Indoor Dust¹³ and House 4: Dripline¹⁴
407 also contain traces of Fe.

408

409 Statements and Declarations

410 **Funding**

411 The Anthropocene Network is supported by the Environmental Resilience Institute, funded by
412 Indiana University’s Prepared for Environmental Change Grand Challenge Initiative. Partial
413 support for this work was provided by NSF-EAR-PF Award #2052589 to M.D.

414 **Competing Interests**

415 The authors have no relevant financial or non-financial interests to disclose.

416 **Author Contributions**

417 **Matthew Dietrich:** Conceptualization, Funding acquisition, Investigation, Methodology,
418 Visualization, Writing – original draft, Data curation. **Shelby T. Rader:** Methodology, Writing –
419 review & editing. **Gabriel M. Filippelli:** Resources, Supervision, Writing – review & editing.

420 **Ethical Approval**

421 “Not applicable”

422

423 **Consent to Participate**

424 “Not applicable”

425

426 **Consent to Publish**

427

428 All authors agree to publish the manuscript in its present form.

429

430 **Availability of data and materials**

431 All data and materials are included in the manuscript and supplementary documentation.

432

433

434 **References**

- 435 Adgate, J., Rhoads, G., & Liroy, P. (1998). The use of isotope ratios to apportion sources of lead
436 in Jersey City, NJ, house dust wipe samples. *The Science of The Total Environment*,
437 221(2–3), 171–180. [https://doi.org/10.1016/S0048-9697\(98\)00282-4](https://doi.org/10.1016/S0048-9697(98)00282-4)
- 438 Ayuso, R. A., & Foley, N. K. (2020). Surface topography, mineralogy, and Pb isotope survey of
439 wheel weights and solder: Source of metal contaminants of roadways and water systems.
440 *Journal of Geochemical Exploration*, 212, 106493.
441 <https://doi.org/10.1016/j.gexplo.2020.106493>
- 442 Barnes, M., McLeod, C. L., Chappell, C., Faraci, O., Gibson, B., & Krekeler, M. P. S. (2020).
443 Characterizing the geogenic background of the Midwest: A detailed mineralogical and
444 geochemical investigation of a glacial till in southwestern Ohio. *Environmental Earth*
445 *Sciences*, 79(6), 159. <https://doi.org/10.1007/s12665-020-8890-z>
- 446 Betts, K. S. (2012). CDC Updates Guidelines for Children’s Lead Exposure. *Environmental*
447 *Health Perspectives*, 120(7). <https://doi.org/10.1289/ehp.120-a268>
- 448 Deniel, C., & Pin, C. (2001). Single-stage method for the simultaneous isolation of lead and
449 strontium from silicate samples for isotopic measurements. *Analytica Chimica Acta*,
450 426(1), 95–103. [https://doi.org/10.1016/S0003-2670\(00\)01185-5](https://doi.org/10.1016/S0003-2670(00)01185-5)
- 451 Dietrich, M., Krekeler, M. P. S., Kousehlar, M., & Widom, E. (2021). Quantification of Pb
452 pollution sources in complex urban environments through a multi-source isotope mixing
453 model based on Pb isotopes in lichens and road sediment. *Environmental Pollution*, 288,
454 117815. <https://doi.org/10.1016/j.envpol.2021.117815>
- 455 Dietrich, M., Shukle, J. T., Krekeler, M. P. S., Wood, L. R., & Filippelli, G. M. (2022). Using
456 Community Science to Better Understand Lead Exposure Risks. *GeoHealth*, 6(2),
457 e2021GH000525. <https://doi.org/10.1029/2021GH000525>

458 Dietrich, M., Wolfe, A., Burke, M., & Krekeler, M. P. S. (2019). The first pollution investigation
459 of road sediment in Gary, Indiana: Anthropogenic metals and possible health implications
460 for a socioeconomically disadvantaged area. *Environment International*, 128, 175–192.
461 <https://doi.org/10.1016/j.envint.2019.04.042>

462 Egendorf, S. P., Gailey, A. D., Schachter, A. E., & Mielke, H. W. (2020). Soil toxicants that
463 potentially affect children’s health. *Current Problems in Pediatric and Adolescent Health*
464 *Care*, 50(1), 100741. <https://doi.org/10.1016/j.cppeds.2019.100741>

465 Filippelli, G. M., Adamic, J., Nichols, D., Shukle, J., & Frix, E. (2018). Mapping the Urban Lead
466 Exposome: A Detailed Analysis of Soil Metal Concentrations at the Household Scale
467 Using Citizen Science. *International Journal of Environmental Research and Public*
468 *Health*, 15(7), 1531. <https://doi.org/10.3390/ijerph15071531>

469 Gaberšek, M., & Gosar, M. (2021). Towards a holistic approach to the geochemistry of solid
470 inorganic particles in the urban environment. *Science of The Total Environment*, 763,
471 144214. <https://doi.org/10.1016/j.scitotenv.2020.144214>

472 Galer, S. J. G., & Abouchami, W. (1998). Practical Application of Lead Triple Spiking for
473 Correction of Instrumental Mass Discrimination. *Mineralogical Magazine*, 62A(1), 491–
474 492. <https://doi.org/10.1180/minmag.1998.62A.1.260>

475 Gillings, M. M., Fry, K. L., Morrison, A. L., & Taylor, M. P. (2022). Spatial distribution and
476 composition of mine dispersed trace metals in residential soil and house dust:
477 Implications for exposure assessment and human health. *Environmental Pollution*, 293,
478 118462. <https://doi.org/10.1016/j.envpol.2021.118462>

479 Hayhow, C., Brabander, D., Jim, R., Lively, M., and Filippelli, G.M. (2021). Addressing the
480 need for just GeoHealth engagement: Evolving models for actionable research that
481 transform communities. *GeoHealth*. <https://doi.org/10.1029/2021GH000496>

482 Hengren, L., Goonetilleke, A., & Ayoko, G. A. (2006). Analysis of heavy metals in road-
483 deposited sediments. *Analytica Chimica Acta*, 571(2), 270–278.
484 <https://doi.org/10.1016/j.aca.2006.04.064>

485 Jaeger, R. J., Weiss, A. L., & Manton, W. I. (1998). Isotopic Ratio Analysis in Residential Lead-
486 Based Paint and Associated Surficial Dust. *Journal of Toxicology: Clinical Toxicology*,
487 36(7), 691–703. <https://doi.org/10.3109/15563659809162617>

488 Kelepertzis, E., Argyraki, A., Chrastný, V., Botsou, F., Skordas, K., Komárek, M., & Fouskas,
489 A. (2020). Metal(loid) and isotopic tracing of Pb in soils, road and house dusts from the
490 industrial area of Volos (central Greece). *Science of The Total Environment*, 725, 138300.
491 <https://doi.org/10.1016/j.scitotenv.2020.138300>

492 Kelepertzis, E., Chrastný, V., Botsou, F., Sigala, E., Kypridou, Z., Komárek, M., Skordas, K.,
493 & Argyraki, A. (2021). Tracing the sources of bioaccessible metal(loid)s in urban
494 environments: A multidisciplinary approach. *Science of The Total Environment*, 771,
495 144827. <https://doi.org/10.1016/j.scitotenv.2020.144827>

496 Kousehlar, M., & Widom, E. (2020). Identifying the sources of air pollution in an urban-
497 industrial setting by lichen biomonitoring—A multi-tracer approach. *Applied*
498 *Geochemistry*, 121, 104695. <https://doi.org/10.1016/j.apgeochem.2020.104695>

499 Laidlaw, M. A. S., & Filippelli, G. M. (2008). Resuspension of urban soils as a persistent source
500 of lead poisoning in children: A review and new directions. *Applied Geochemistry*, 23(8),
501 2021–2039. <https://doi.org/10.1016/j.apgeochem.2008.05.009>

502 Miler, M., & Gosar, M. (2019). Assessment of contribution of metal pollution sources to attic
503 and household dust in Pb-polluted area. *Indoor Air*, 29(3), 487–498.
504 <https://doi.org/10.1111/ina.12548>

505 Obeng-Gyasi, E., Roostaei, J., & Gibson, J. M. (2021). Lead Distribution in Urban Soil in a
506 Medium-Sized City: Household-Scale Analysis. *Environmental Science & Technology*,
507 55(6), 3696–3705. <https://doi.org/10.1021/acs.est.0c07317>

508 Rader, S. T., Gaschnig, R. M., Newby, S. M., Bebout, G. E., Mirakian, M. J., & Owens, J. D.
509 (2021). Thallium behavior during high-pressure metamorphism in the Western Alps,
510 Europe. *Chemical Geology*, 579, 120349. <https://doi.org/10.1016/j.chemgeo.2021.120349>

511 Resongles, E., Dietze, V., Green, D. C., Harrison, R. M., Ochoa-Gonzalez, R., Tremper, A. H., &
512 Weiss, D. J. (2021). Strong evidence for the continued contribution of lead deposited
513 during the 20th century to the atmospheric environment in London of today. *Proceedings*
514 *of the National Academy of Sciences*, 118(26). <https://doi.org/10.1073/pnas.2102791118>

515 Ringwald, P., Chapin, C., Iceman, C., Tighe, M. E., Sisk, M., Peaslee, G. F., Peller, J., & Wells,
516 E. M. (2021). Characterization and within-site variation of environmental metal
517 concentrations around a contaminated site using a community-engaged approach.
518 *Chemosphere*, 272, 129915. <https://doi.org/10.1016/j.chemosphere.2021.129915>

519 Smith, D.B., Cannon, W.F., Woodruff, L.G., Solano, Federico, Kilburn, J.E., and Fey, D.L.,
520 (2013). Geochemical and mineralogical data for soils of the conterminous United States:
521 U.S. Geological Survey Data Series 801, 19 p., <https://pubs.usgs.gov/ds/801/>.

522 Sutherland, R. A., Day, J. P., & Bussen, J. O. (2003). Lead Concentrations, Isotope Ratios, and
523 Source Apportionment in Road Deposited Sediments, Honolulu, Oahu, Hawaii. *Water,*
524 *Air, and Soil Pollution*, 142, 165–186.

525 Tansel, B., & Rafiuddin, S. (2016). Heavy metal content in relation to particle size and organic
526 content of surficial sediments in Miami River and transport potential. *International*
527 *Journal of Sediment Research*, 31(4), 324–329.
528 <https://doi.org/10.1016/j.ijsrc.2016.05.004>

529 Thibodeau, A. M., Killick, D. J., Ruiz, J., Chesley, J. T., Deagan, K., Cruxent, J. M., & Lyman,
530 W. (2007). The strange case of the earliest silver extraction by European colonists in the
531 New World. *Proceedings of the National Academy of Sciences*, 104(9), 3663–3666.
532 <https://doi.org/10.1073/pnas.0607297104>

533 Wade, A. M., Richter, D. D., Craft, C. B., Bao, N. Y., Heine, P. R., Osteen, M. C., & Tan, K. G.
534 (2021). Urban-Soil Pedogenesis Drives Contrasting Legacies of Lead from Paint and
535 Gasoline in City Soil. *Environmental Science & Technology*, 55(12), 7981–7989.
536 <https://doi.org/10.1021/acs.est.1c00546>

537 Wang, Z., Dwyer, G. S., Coleman, D. S., & Vengosh, A. (2019). Lead Isotopes as a New Tracer
538 for Detecting Coal Fly Ash in the Environment. *Environmental Science & Technology*
539 *Letters*, 6(12), 714–719. <https://doi.org/10.1021/acs.estlett.9b00512>

540 Wang, Z., Wade, A. M., Richter, D. D., Stapleton, H. M., Kaste, J. M., & Vengosh, A. (2021).
541 Legacy of anthropogenic lead in urban soils: Co-occurrence with metal(loids) and fallout
542 radionuclides, isotopic fingerprinting, and in vitro bioaccessibility. *Science of The Total*
543 *Environment*, 151276. <https://doi.org/10.1016/j.scitotenv.2021.151276>

544 Watson, G. P., Martin, N. F., Grant, Z. B., Batka, S. C., & Margenot, A. J. (2022). Soil lead
545 distribution in Chicago, USA. *Geoderma Regional*, 28, e00480.
546 <https://doi.org/10.1016/j.geodrs.2021.e00480>

547

Supplementary Information

Using community science for detailed pollution research: A case-study approach in Indianapolis, IN, USA

Matthew Dietrich^{1*}, Shelby Rader², Gabriel Filippelli^{1,3}

¹Department of Earth Sciences, Indiana University – Purdue University Indianapolis, Indianapolis, IN, USA

²Department of Earth and Atmospheric Sciences, Indiana University, Bloomington, IN, USA

³Environmental Resilience Institute, Indiana University, Bloomington, IN, USA

*Corresponding Author: mjdietri@iu.edu

Supplementary Text

Test S1-Instrument Analyses

The Pb isotopes ²⁰⁴Pb, ²⁰⁶Pb, ²⁰⁷Pb, and ²⁰⁸Pb were detected along with ²⁰²Hg, ²⁰³Tl, and ²⁰⁵Tl with a Nu Plasma II Multicollector Inductively Coupled Plasma Mass Spectrometer (MC-ICP-MS). All Pb isotope results were Hg-corrected, albeit the Hg correction was nominally zero, and corrected on-line for mass discrimination using the known Tl ratio of the NIST 997 spike. All results were then normalized offline to values reported by Galer and Abouchami (1998) for the NIST 981 standard (²⁰⁶Pb/²⁰⁴Pb = 16.9405, ²⁰⁷Pb/²⁰⁴Pb = 15.4963, and ²⁰⁸Pb/²⁰⁴Pb = 36.7219). The errors are derived from the reproducibility of the NIST 981 Pb standard over the course of the run.

Text S2-Quality Control

To address any possible metal contamination through sieving the household soil and dust samples, 5 subsamples of NIST SRM 2702 – Inorganics in Marine Sediment were processed through either dust sieves (NIST_2702_1 and NIST_2702_2) or a 2 mm soil sieve (remaining SRM 2702 samples), as well as through the rest of the sample prep (i.e., digestions). The elements Cd, Tl, Pb, and Sb were deemed acceptable based on mean % recoveries between 80-106% (Table S1), and Pb isotopic contamination was deemed minimal based on low standard deviations for all isotope ratios within the SRM 2702 samples (Table S2), and good agreement with the peer review published ²⁰⁷Pb/²⁰⁶Pb avg value of 0.8377 (calculated from ²⁰⁶Pb/²⁰⁷Pb ratio of 1.1937 for SRM 2702; Jeong et al., 2021—99.62% similarity of our mean ratio to the published ratio).

As a quality control check on sample preparation and analysis, ICP-MS samples included periodic blanks run between samples, which confirmed background levels negligible. Isotopic

35 analyses via MC-ICP-MS included the analysis of a USGS reference material (AGV-2a),
36 prepared and processed as an unknown sample, which was in agreement with previously
37 published isotopic compositions (Table S2), and multiple analyses of an unknown sample during
38 the analytical session (within analytical error of one another), which confirmed instrument
39 stability across the analysis period.

40

41

42

Supplementary Figures

43

44

45

46

47

48

49

50

51

52

53

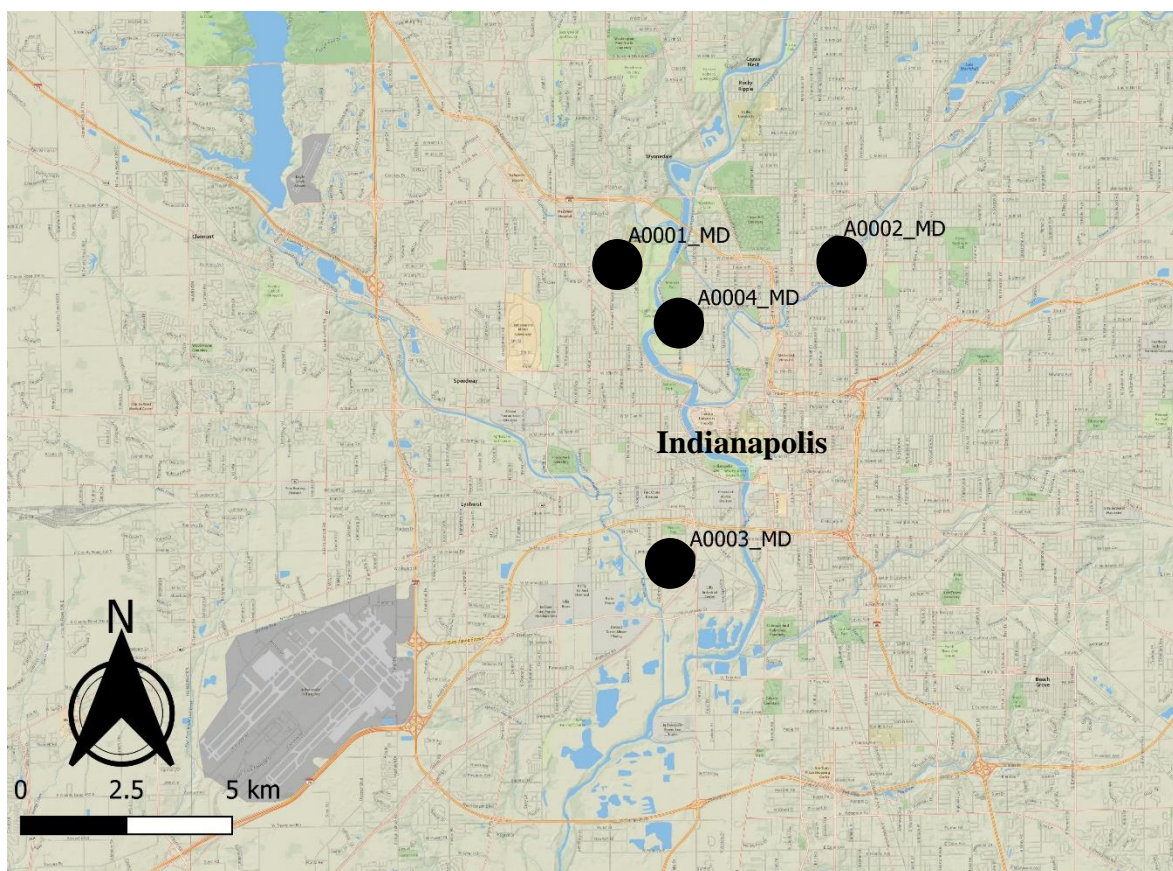
54

55

56

57

58



59 **Fig. S1:** Locations of the homes that provides samples, with symbol size enlarged and the map
60 zoomed out to protect privacy.

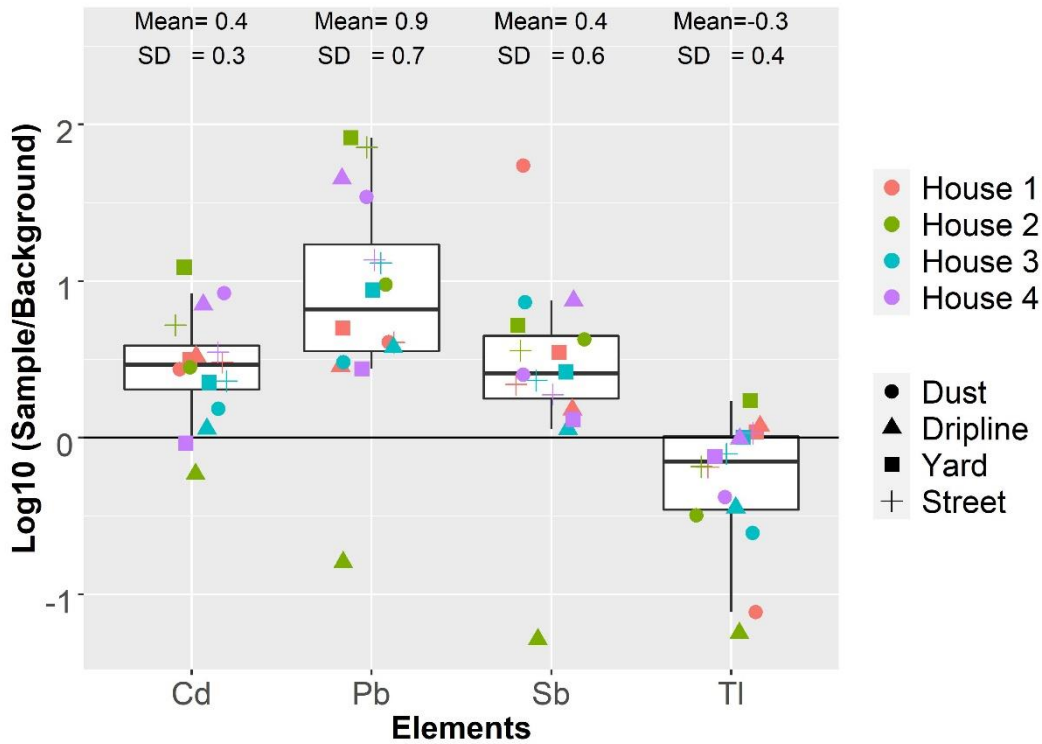
61

62

63

64

65
66
67
68
69
70
71



84

85 **Fig. S2:** Bulk metal concentrations of dust and soil samples normalized to the 75th percentile of
86 Indiana top 0-5cm background soil values from Smith et al. (2013). All values >0 represent
87 enrichment relative to the 75th percentile of background soil metal concentrations in Indiana,
88 U.S.

89
90
91
92
93

94
95
96
97
98
99
100
101
102
103
104
105
106
107
108
109
110
111
112
113
114
115
116
117
118
119
120
121

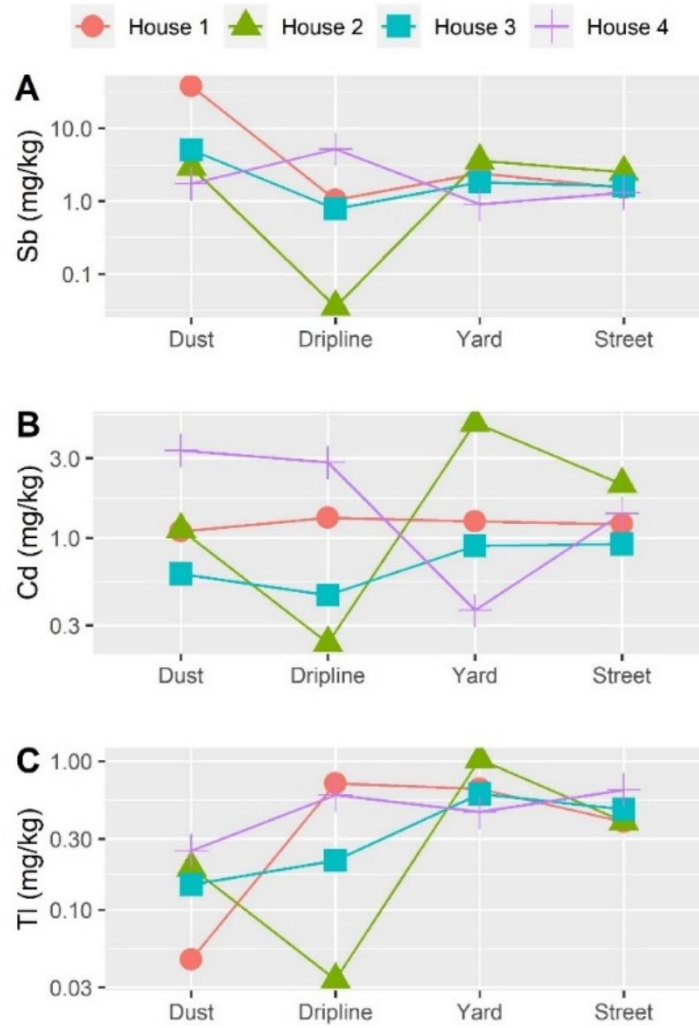


Fig S3: Bulk metal concentrations (mg/kg) for each household based on sampling location.

122
123
124
125
126
127
128
129
130
131
132
133
134
135
136
137
138
139
140
141
142

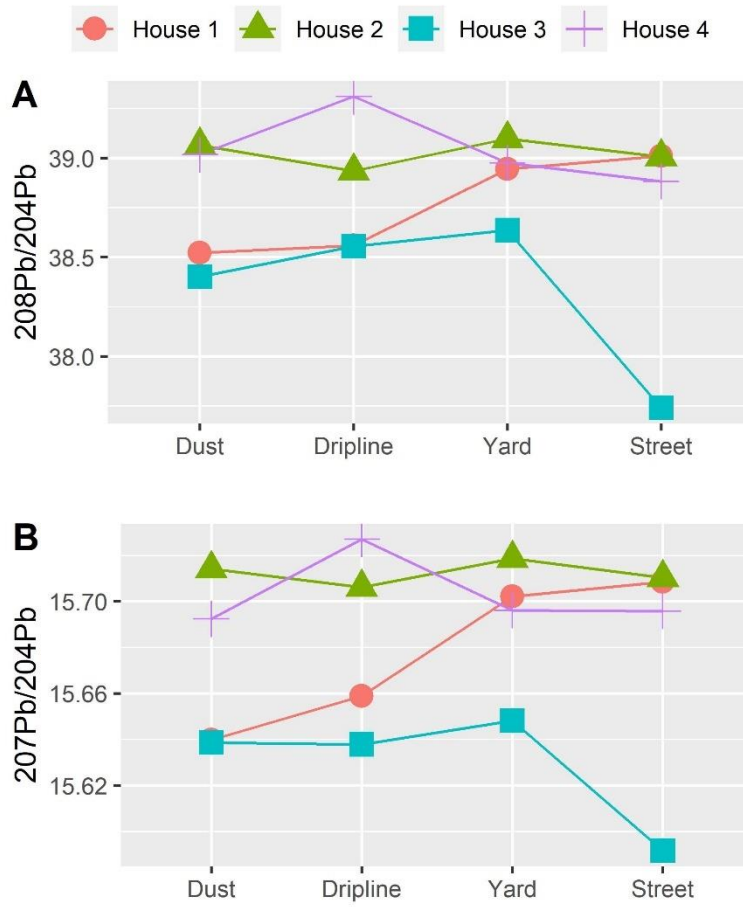
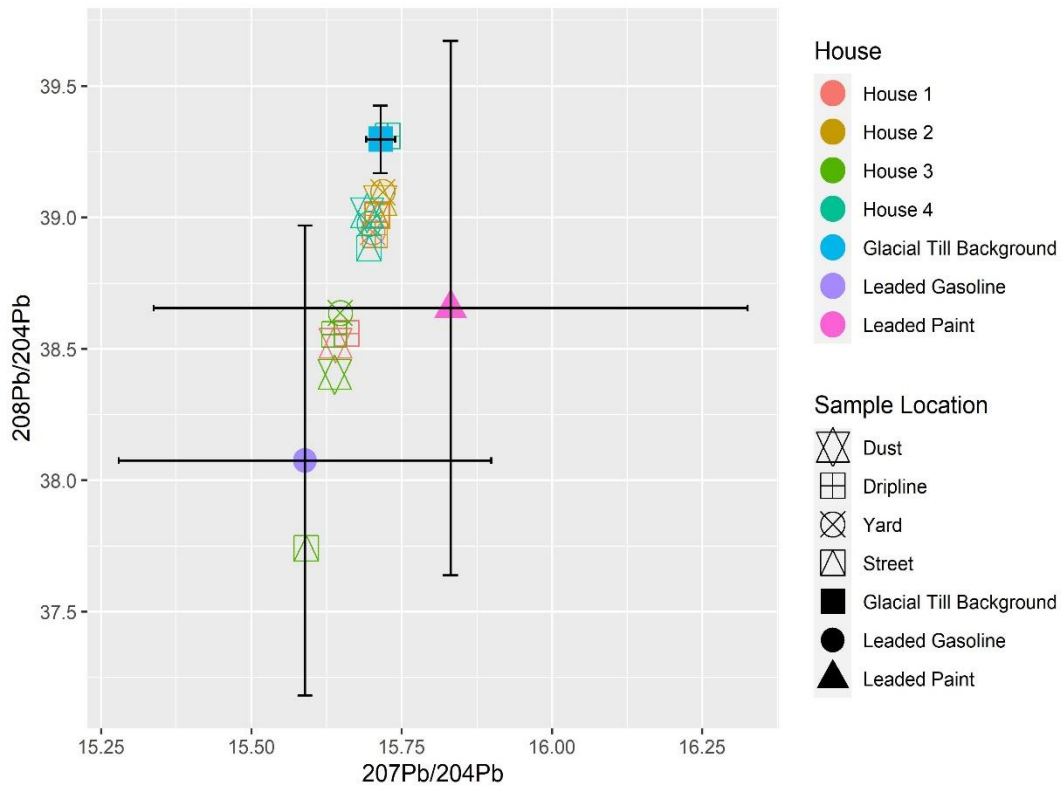
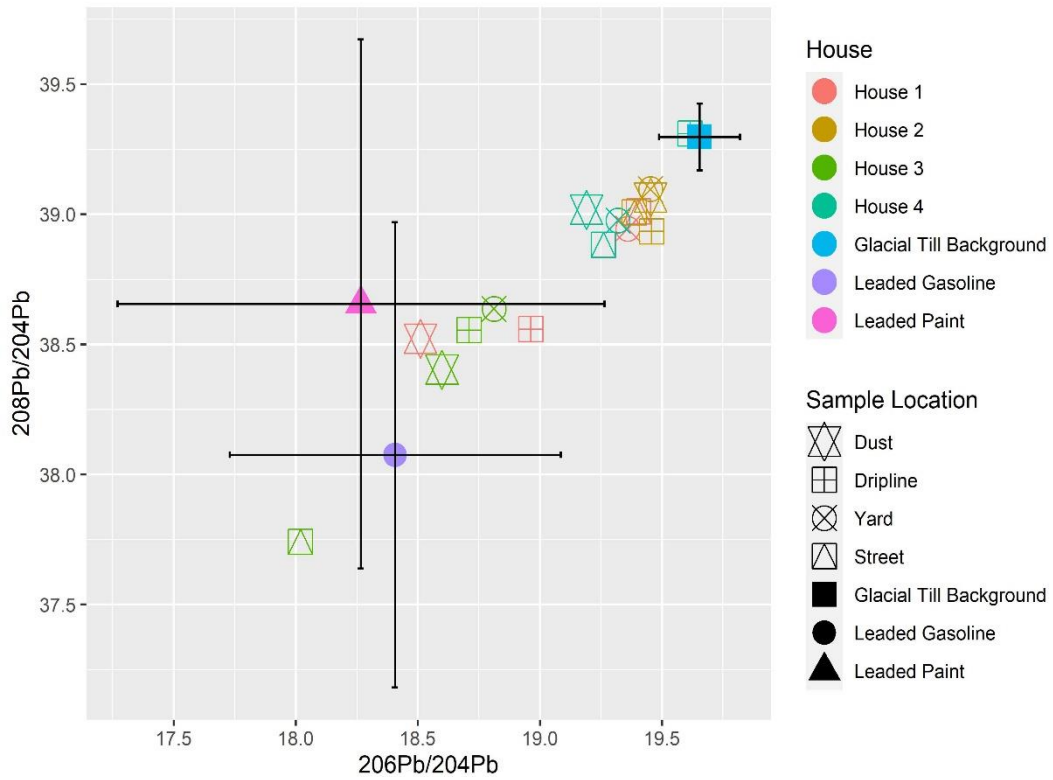


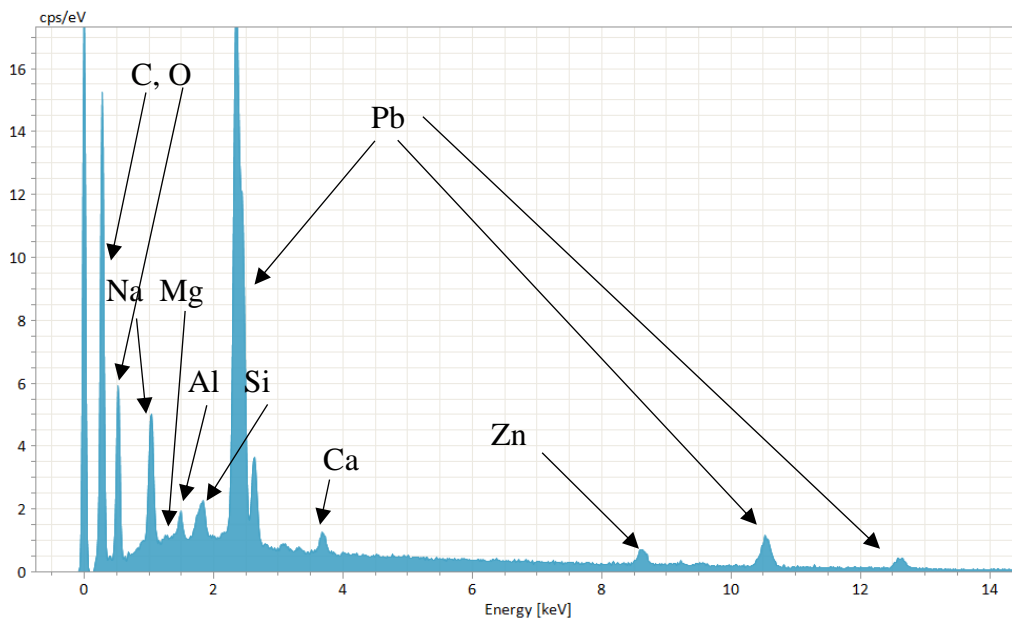
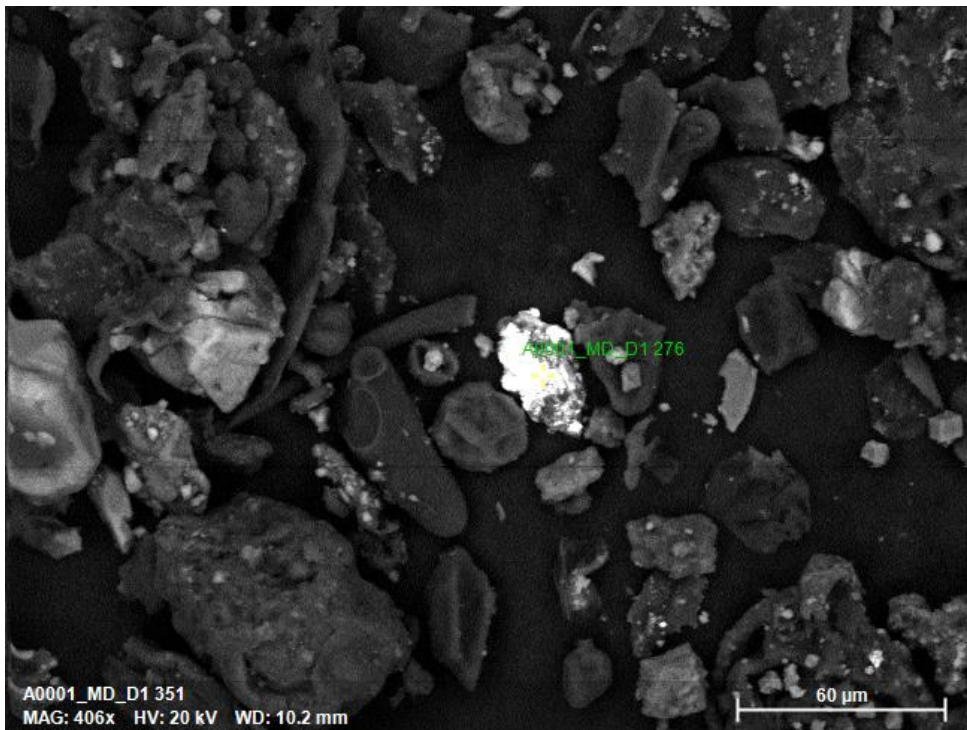
Fig. S4: Additional Pb isotope plots for each household based on sampling location.



169 **Fig. S5:** Bivariate plots of Pb isotopic ratios for all samples and main potential pollution source
 170 endmembers, with error bars representing 1σ variability in the source endmembers (Midwest

171 U.S. Glacial Till/Soil Background—Kousehlar and Widom, 2020, LeGalley et al., 2013; U.S.
172 Leaded Gasoline—Dietrich et al., 2021 and the references therein; Leaded Paint—Wang et al.,
173 2019 and the references therein). 2σ sample analytical variability is minimal relative to the
174 symbol sizes, and thus only displayed in Table S2.

175
176
177
178
179
180
181
182
183
184
185
186



198

199 **Fig. S6:** EDS spot analysis of House 1: Indoor Dust¹.

200
201
202
203
204
205
206
207
208
209
210
211
212
213
214
215
216
217
218
219
220
221
222
223
224
225
226
227

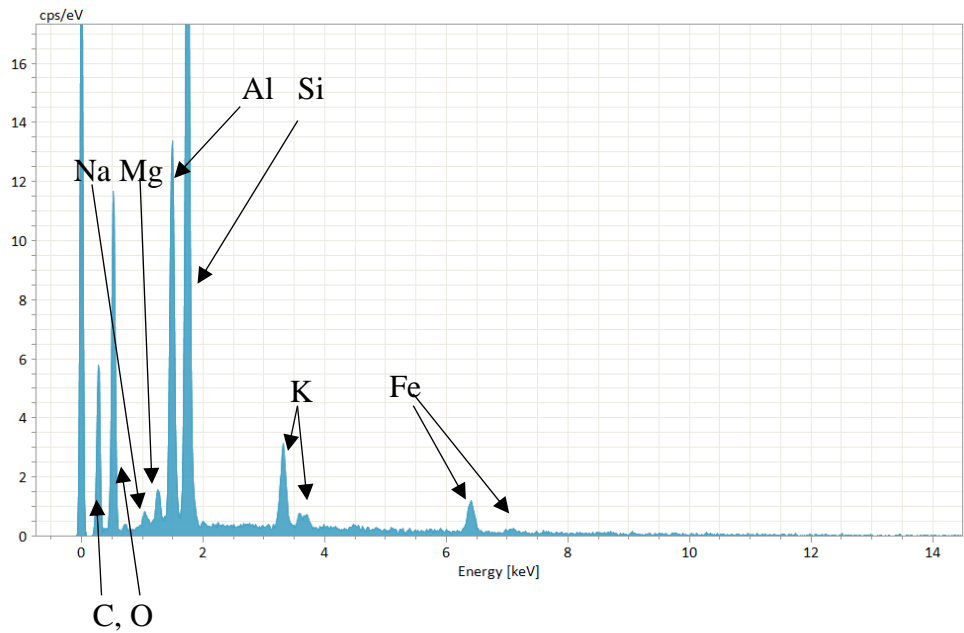
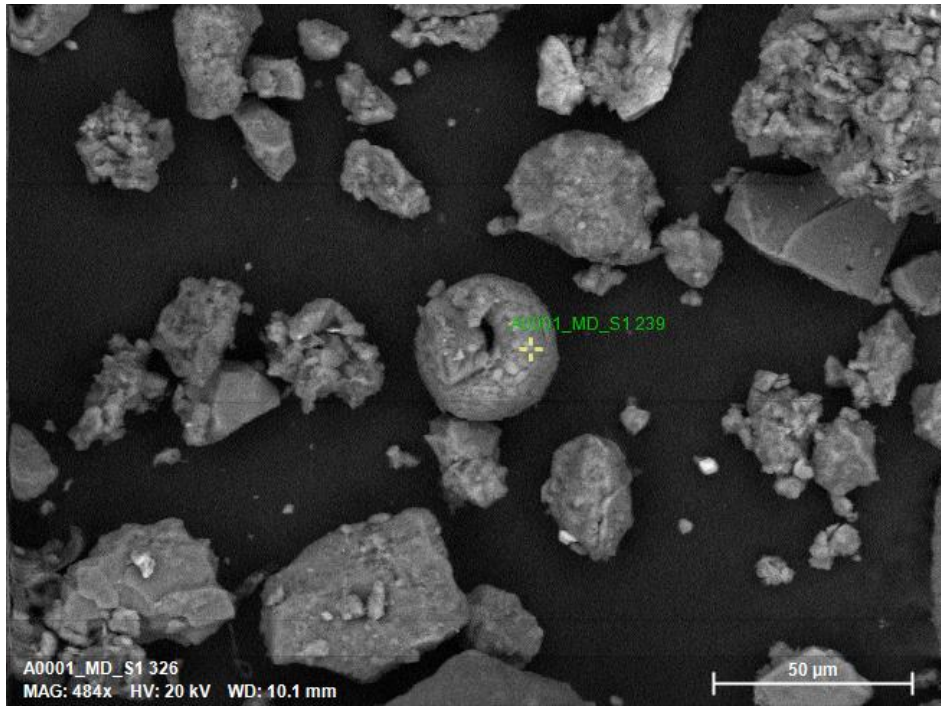


Fig. S7: EDS spot analysis of House 1: Dripline².

228

229

230

231

232

233

234

235

236

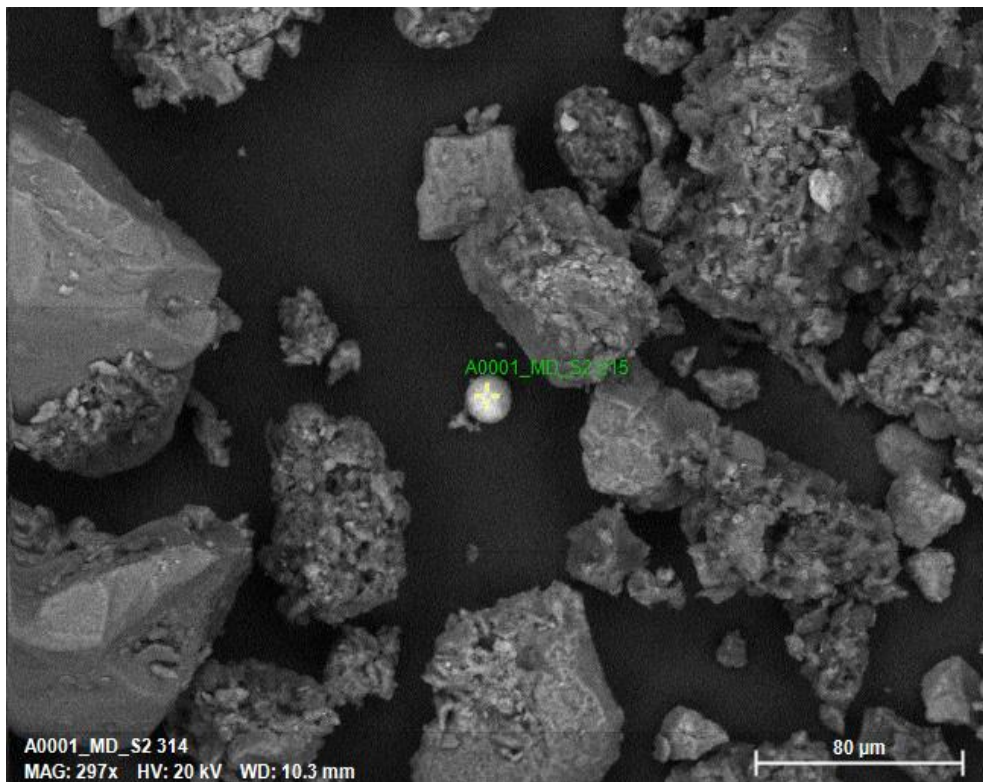
237

238

239

240

241



242

243

244

245

246

247

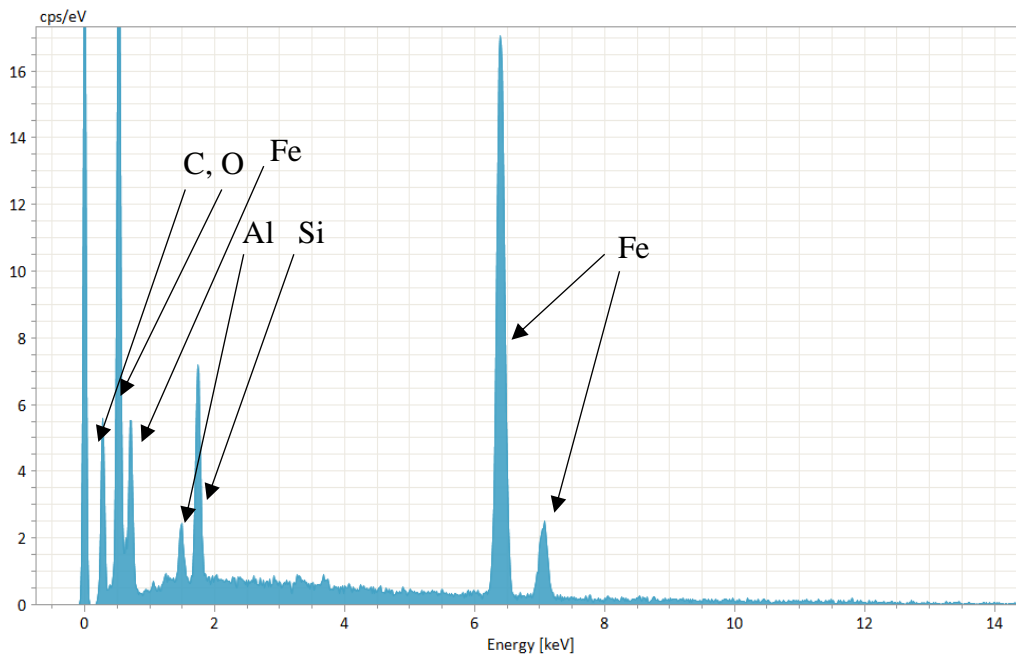
248

249

250

251

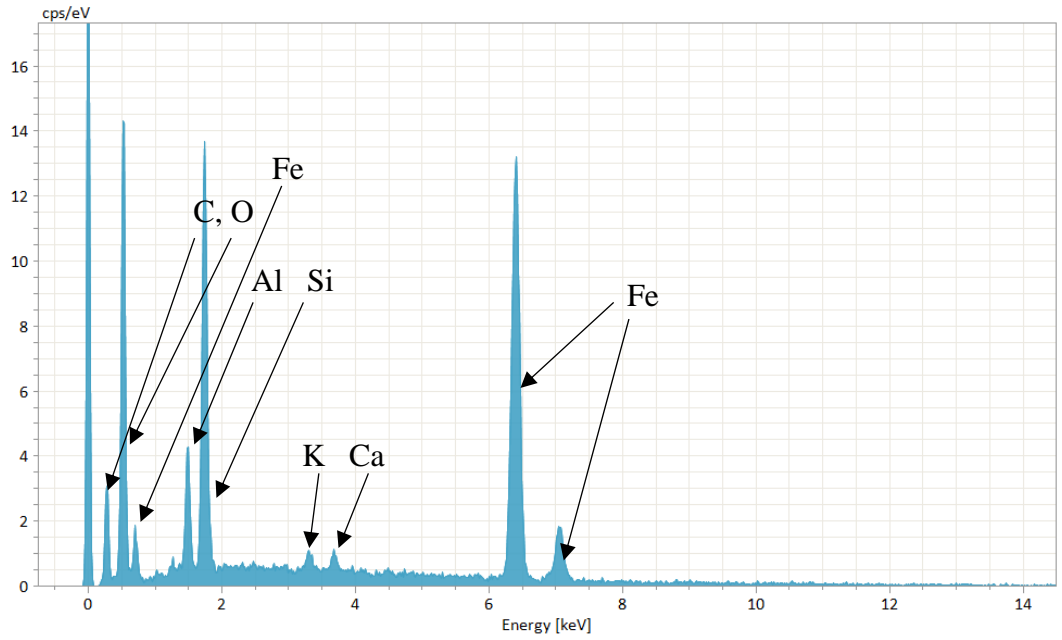
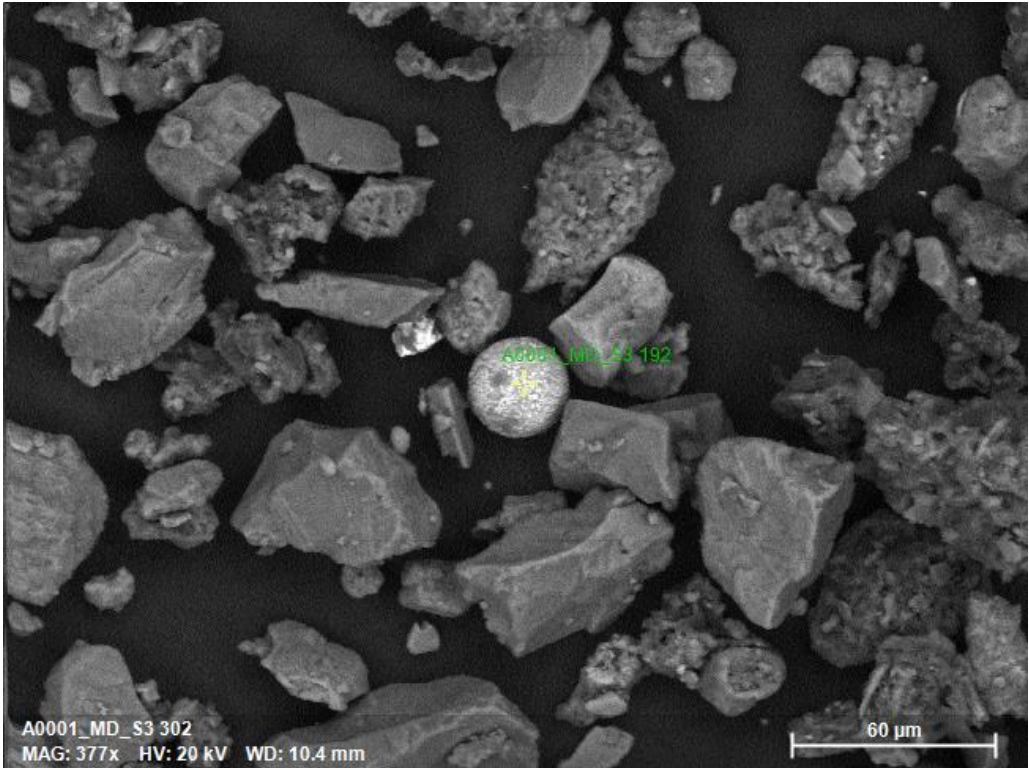
252



253 **Fig. S8:** EDS spot analysis of House 1: Streetside³.

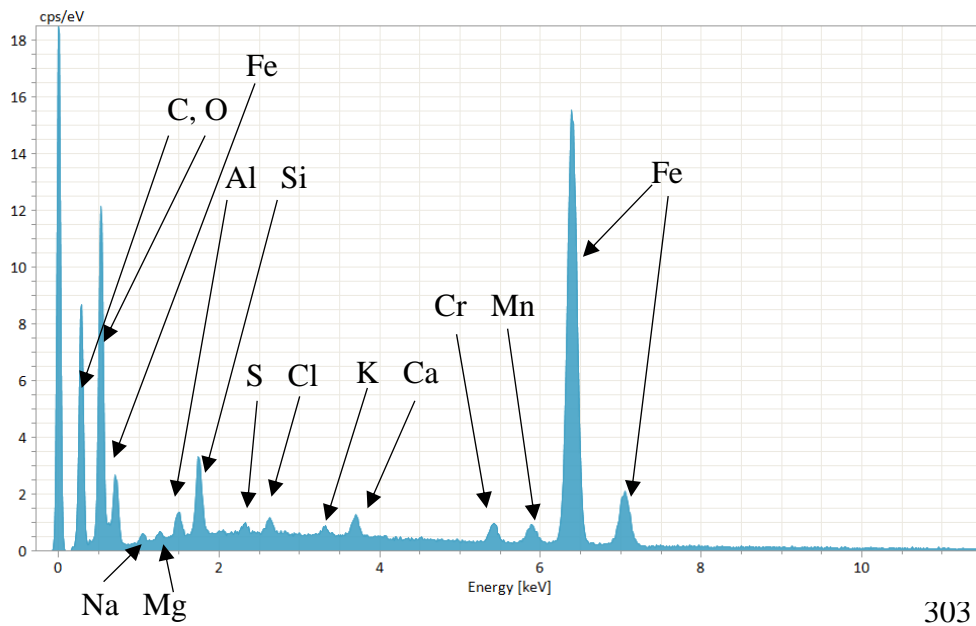
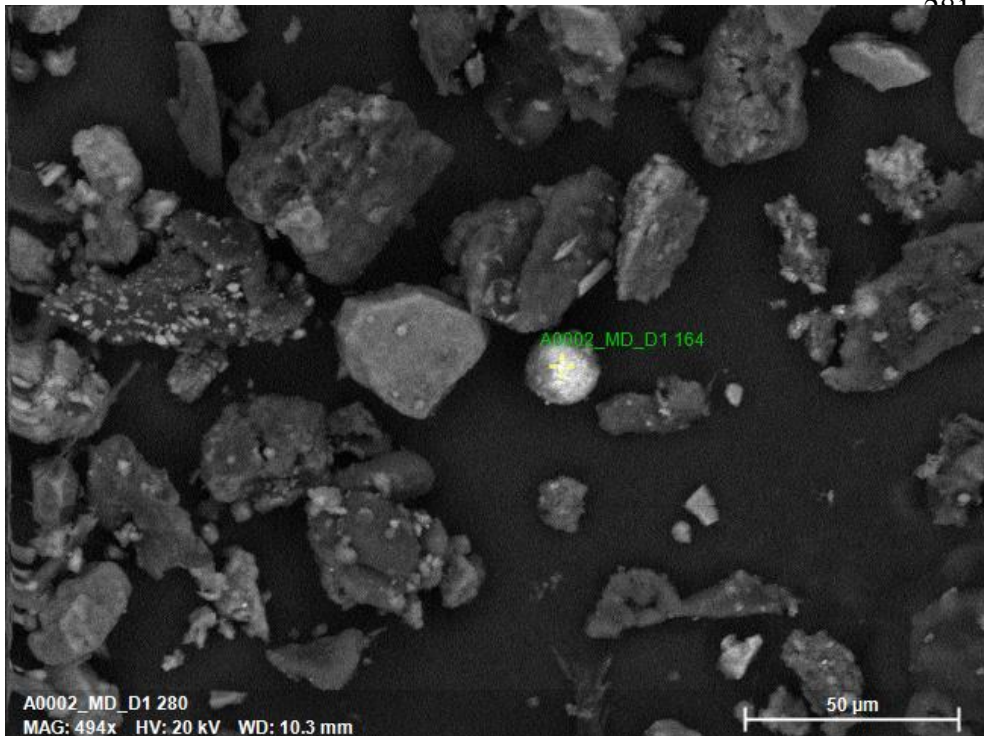
254

255
256
257
258
259
260
261
262
263
264
265
266



278

279 **Fig. S9:** EDS spot analysis of House 1: Yard⁴.
280



304

305 **Fig. S10:** EDS spot analysis of House 2: Indoor Dust⁵.

306

307

308

309
310
311
312
313
314
315
316
317
318
319
320
321
322
323
324
325
326
327
328
329
330
331
332
333
334
335

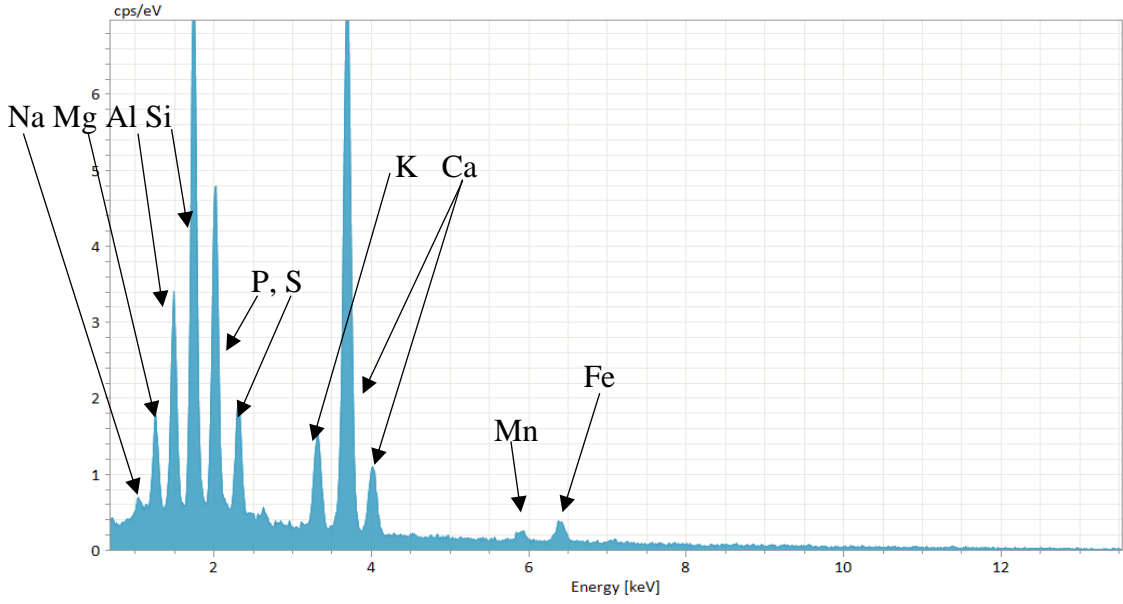
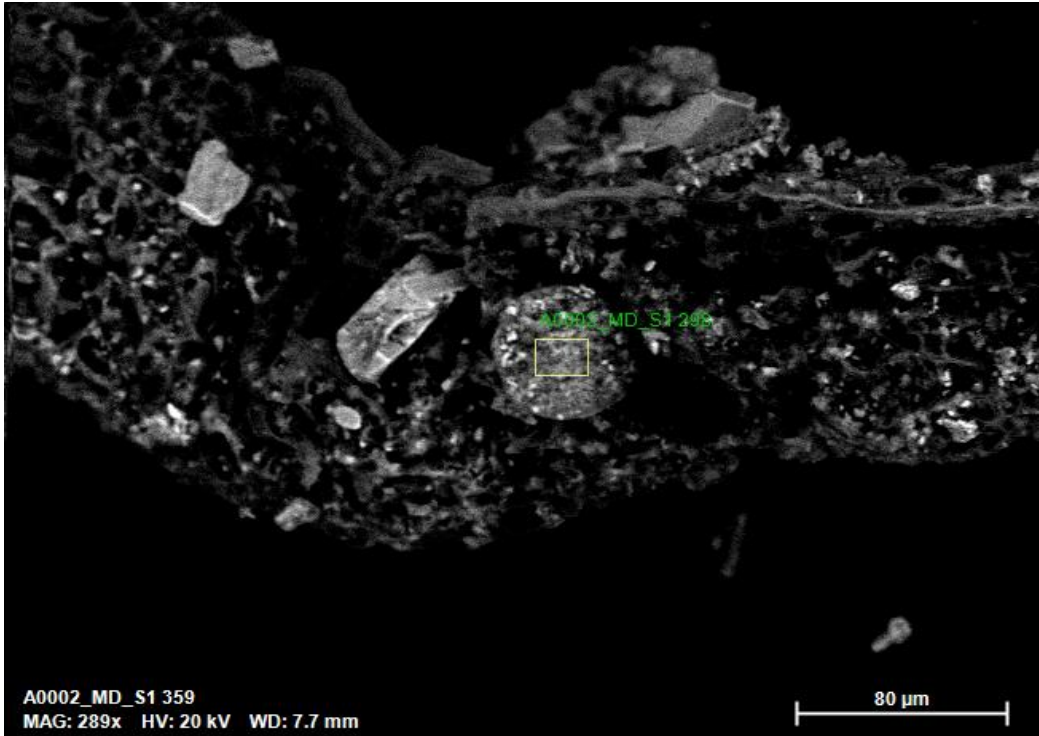


Fig. S11: EDS spot analysis of House 2: Dripline⁶.

336
337
338
339
340
341
342
343
344
345
346
347
348
349
350
351
352
353
354
355
356
357
358
359
360
361
362
363

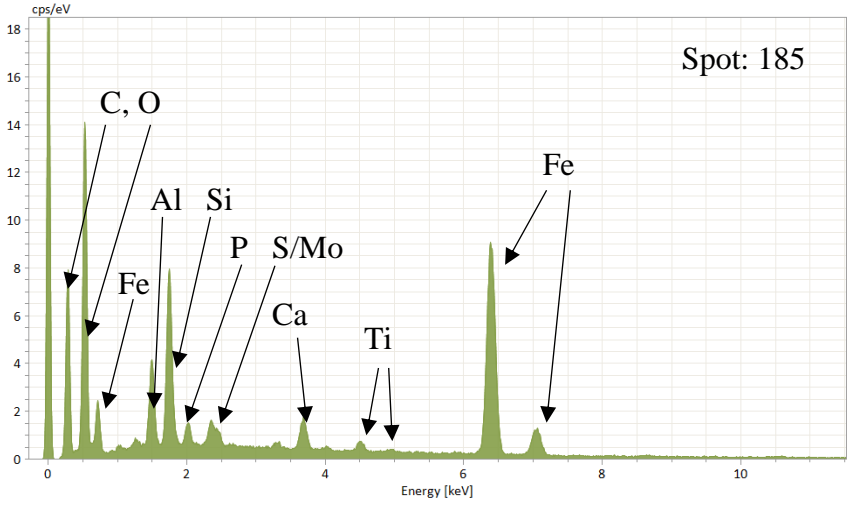
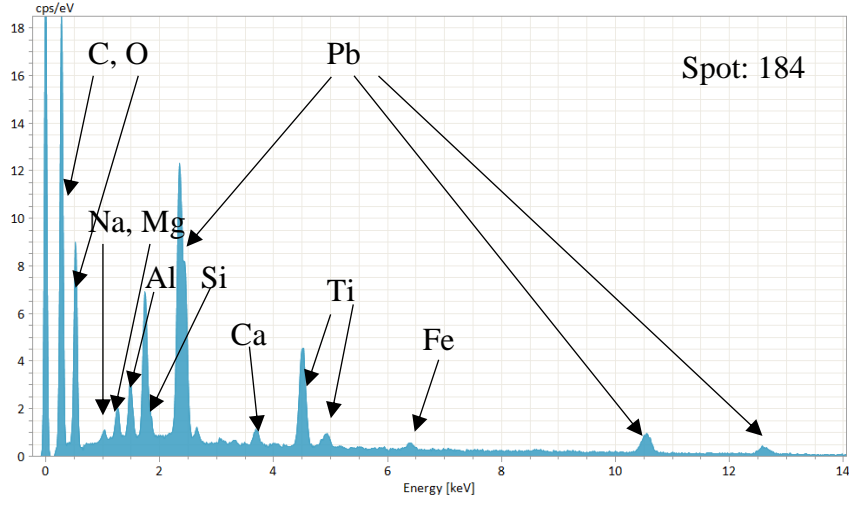
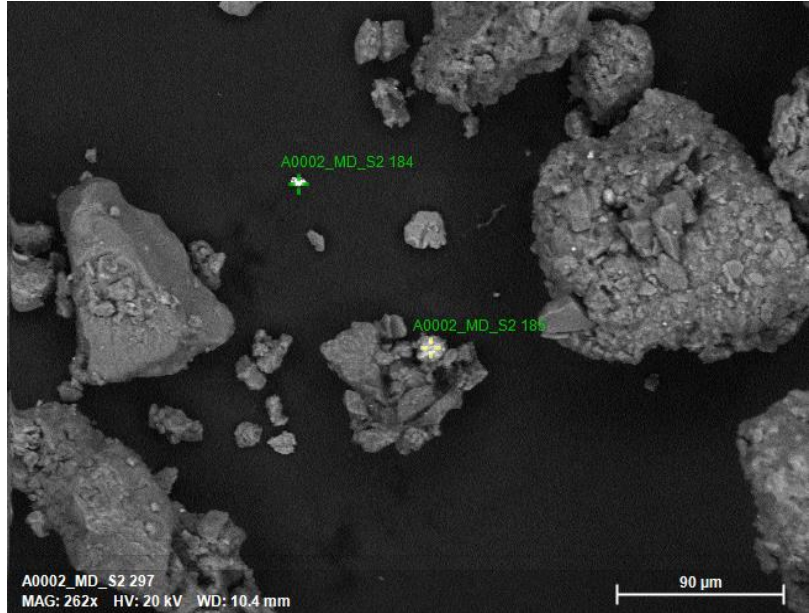
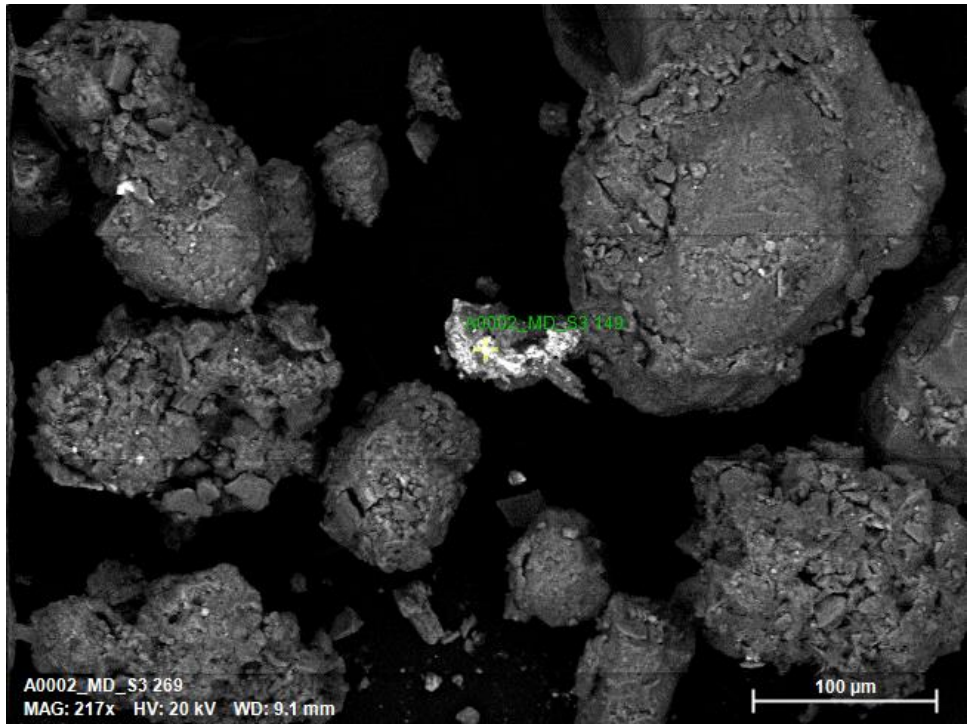
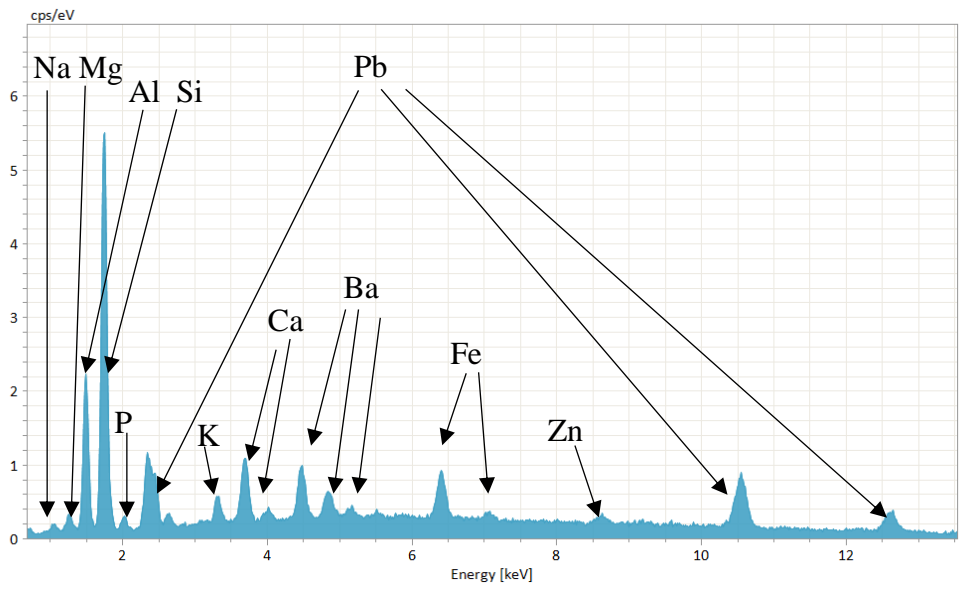


Fig. S12: EDS spot analyses of House 2: Streetside⁷.

364
365
366
367
368
369
370
371
372
373
374
375
376

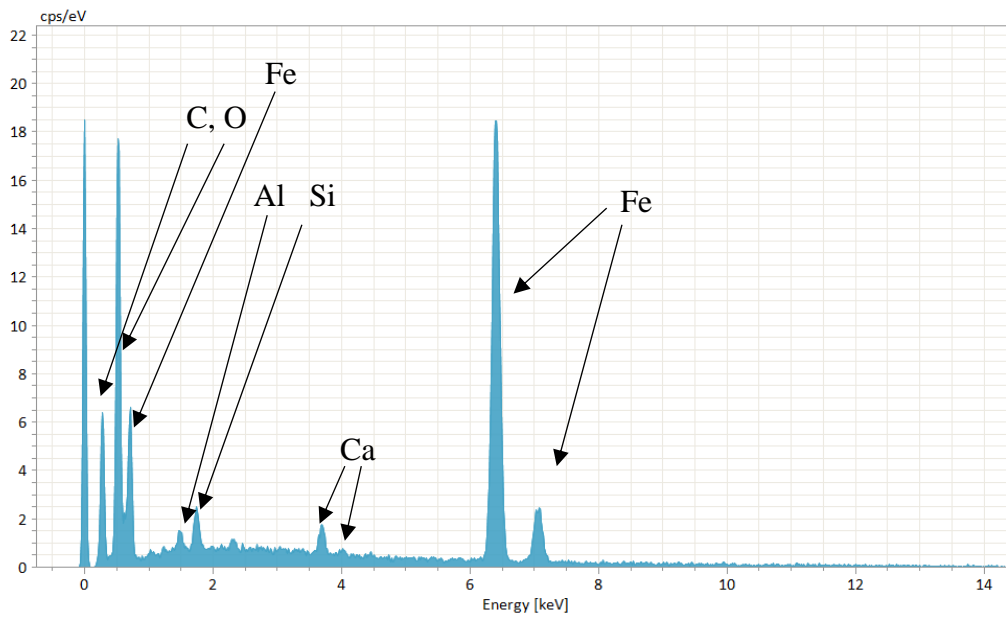
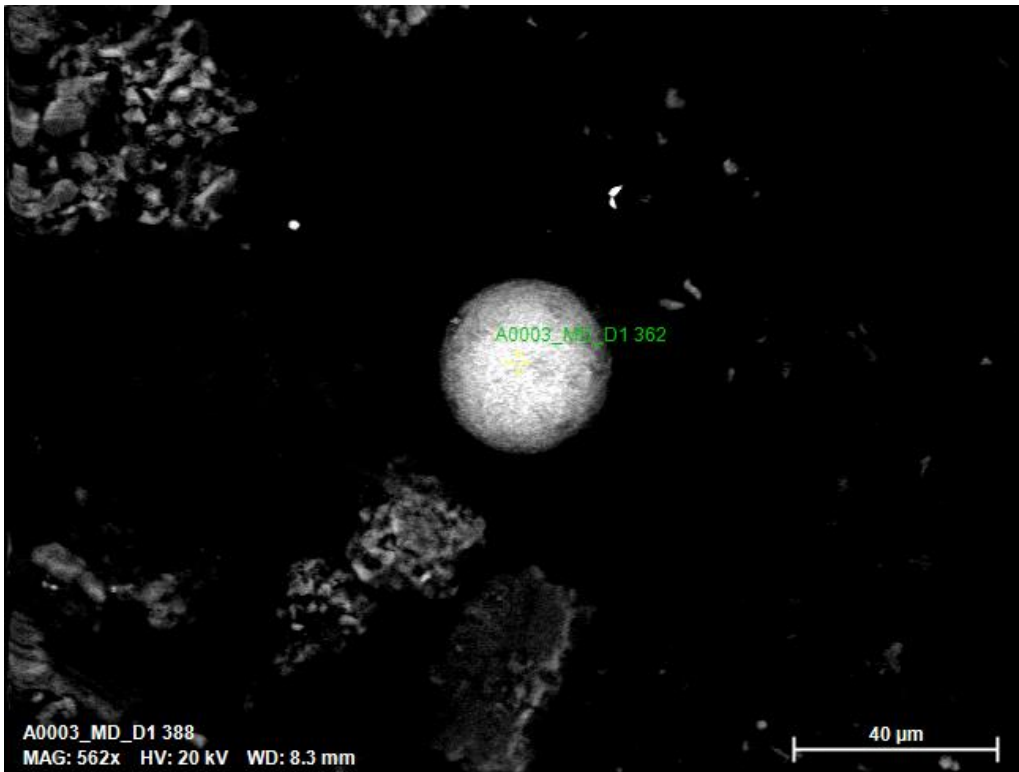


377
378
379
380
381
382
383
384
385
386



387
388
389
390
391

Fig. S13: EDS spot analysis of House 2: Yard⁸.



415

416 **Fig. S14:** EDS spot analysis of House 3: Indoor Dust⁹.

417

418
419
420
421
422
423
424
425
426
427
428
429
430
431
432
433
434
435
436
437
438
439
440
441
442
443

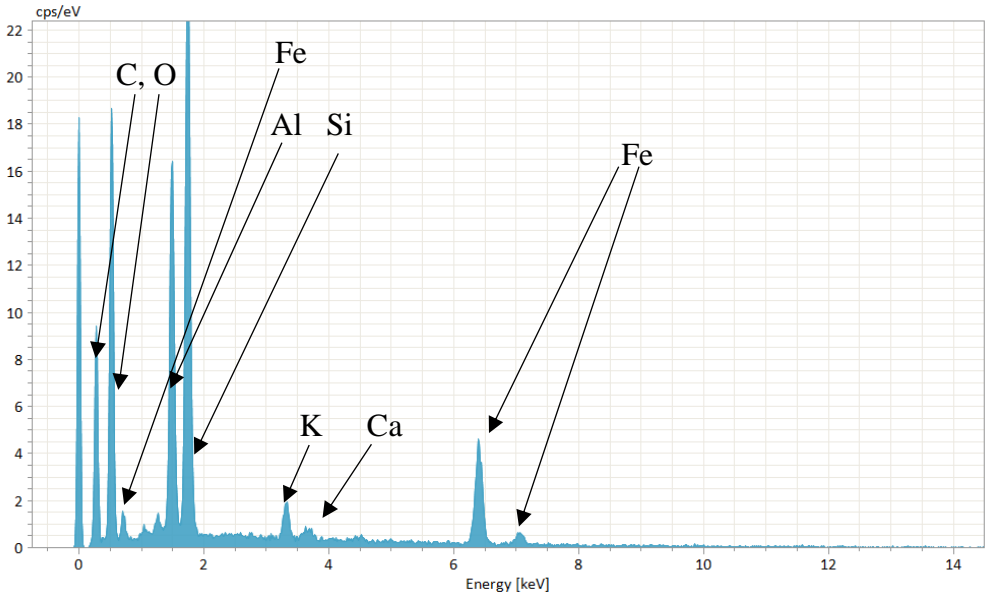
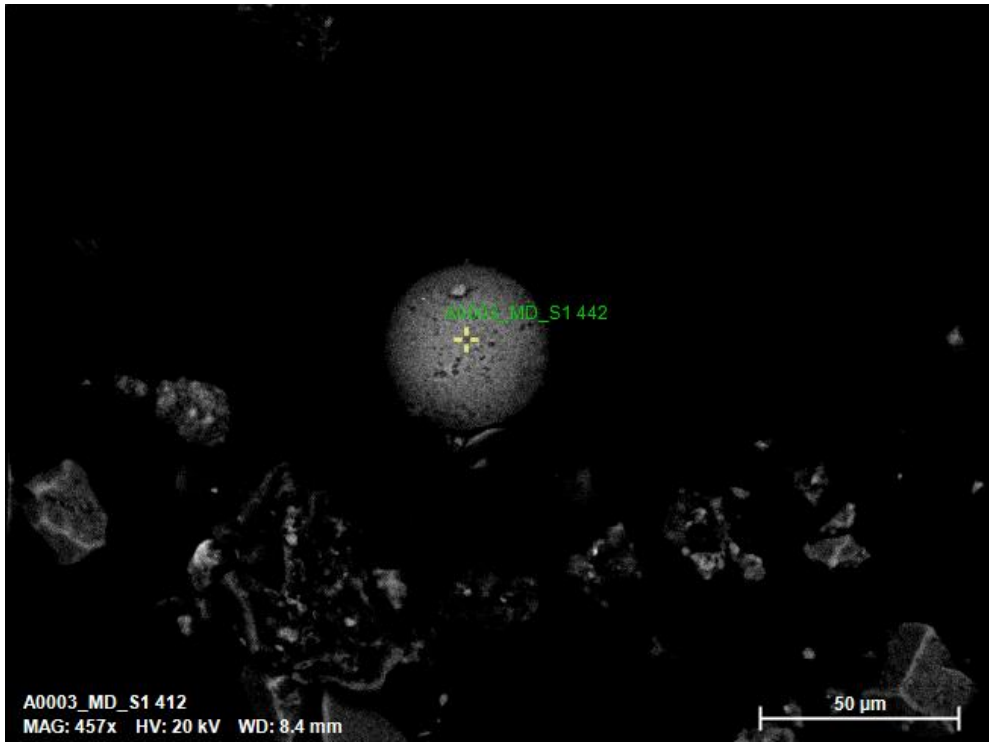
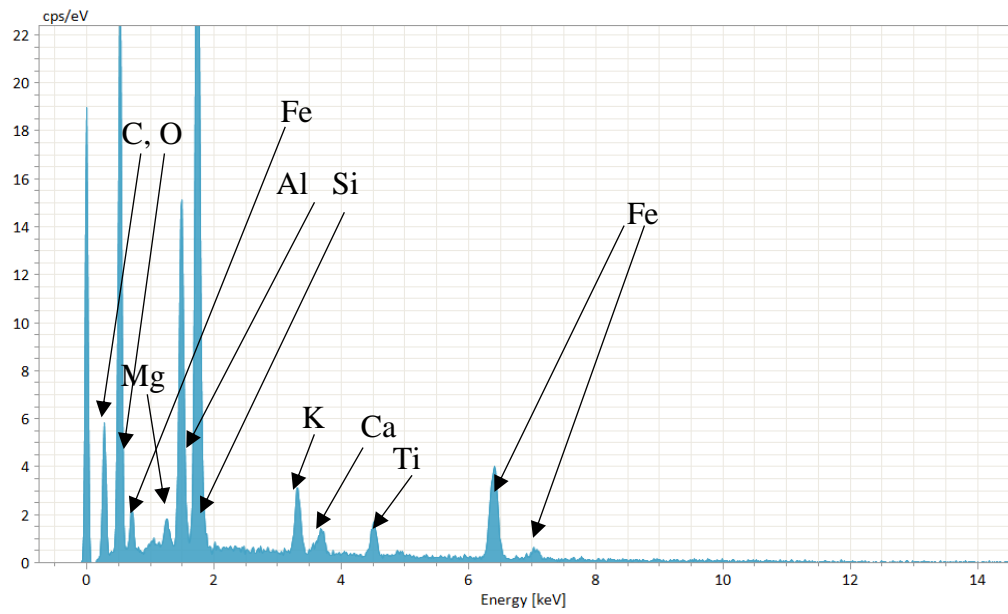
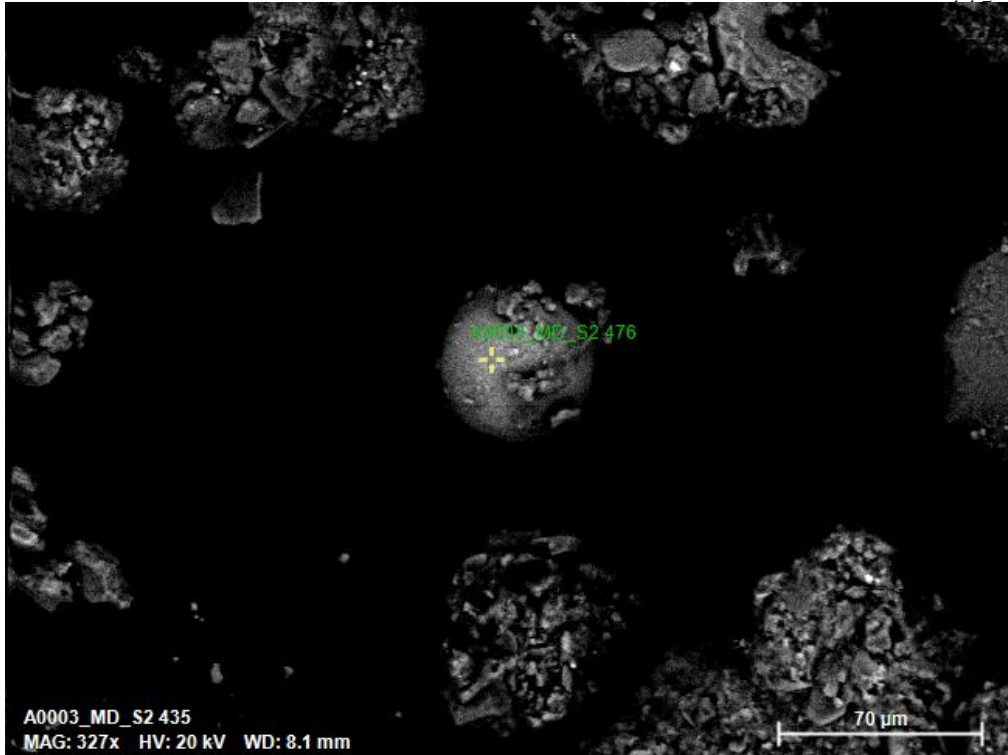


Fig. S15: EDS spot analysis of House 3: Dripline¹⁰.



468 **Fig. S16:** EDS spot analysis of House 3: Streetside¹¹.

469

470
471
472
473
474
475
476
477
478
479
480
481
482
483
484
485
486
487
488
489
490
491
492
493
494
495
496

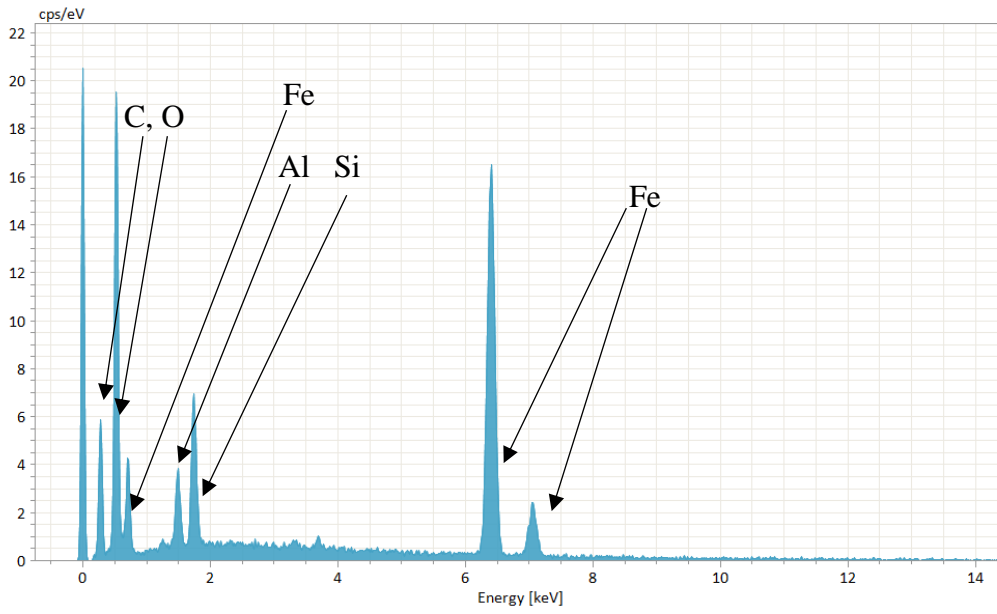
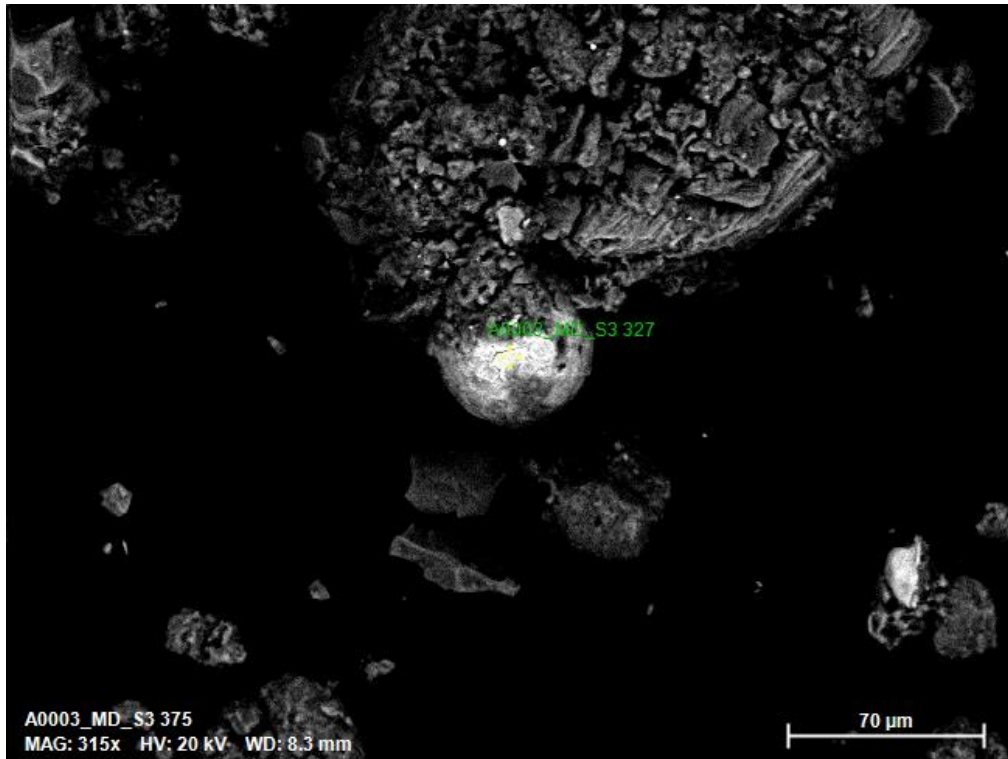


Fig. S17: EDS spot analysis of House 3: Yard¹².

497

498

499

500

501

502

503

504

505

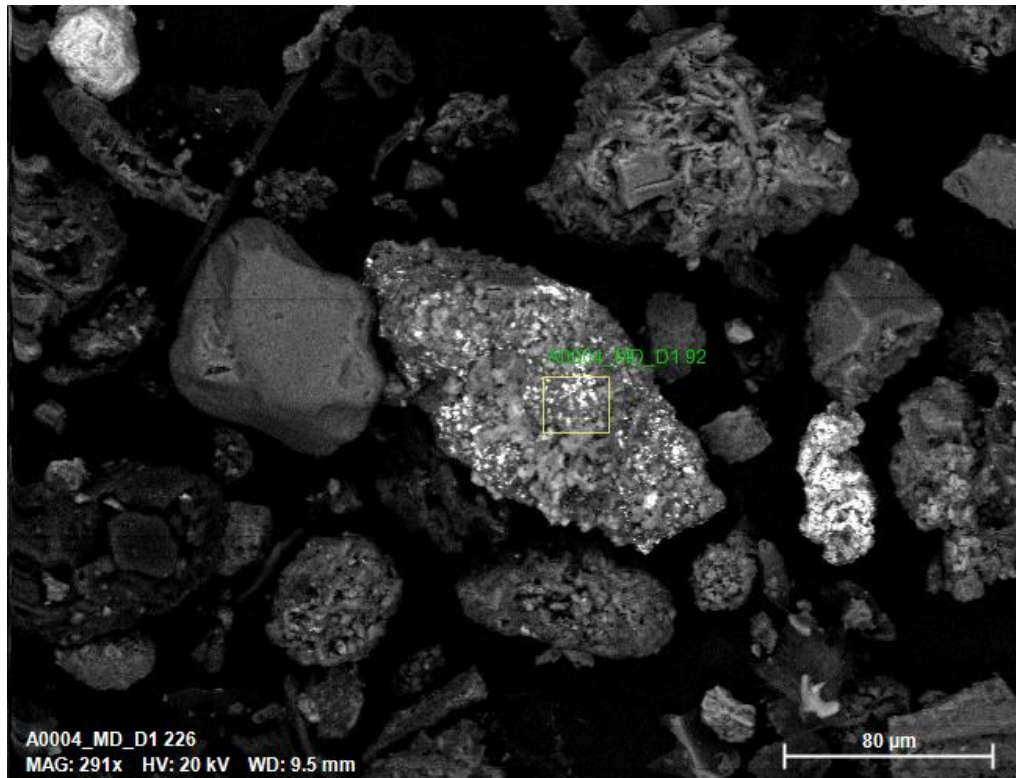
506

507

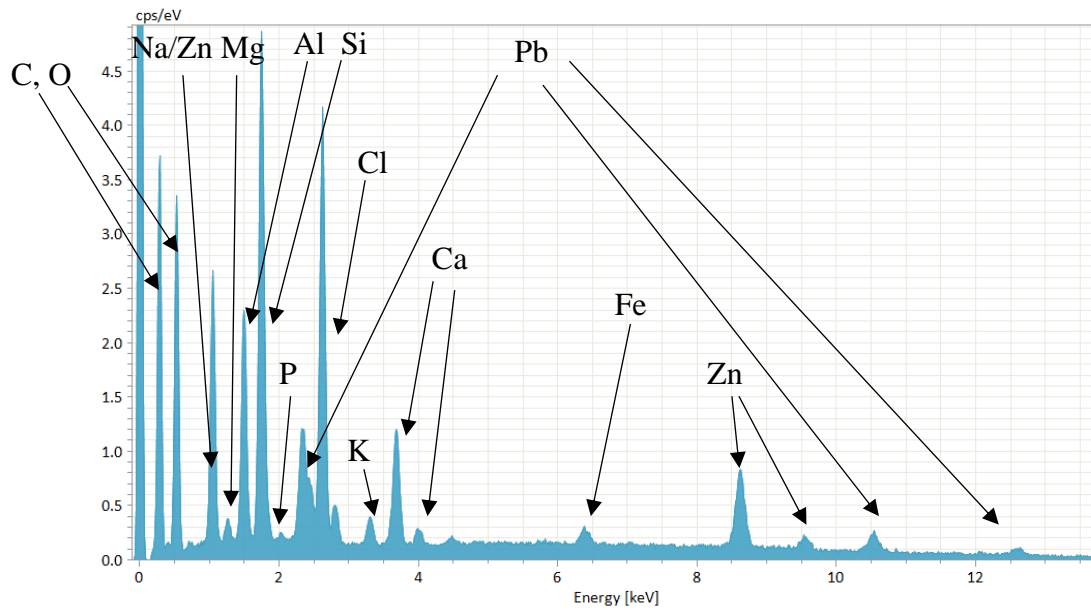
508

509

510



511



520

521

522

523

Fig. S18: EDS spot analysis of House 4: Indoor Dust¹³.

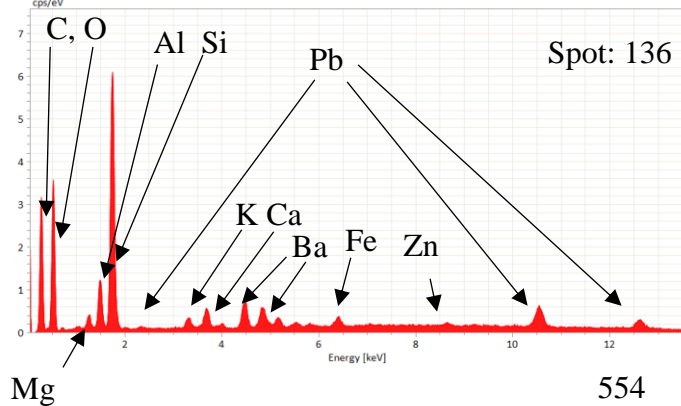
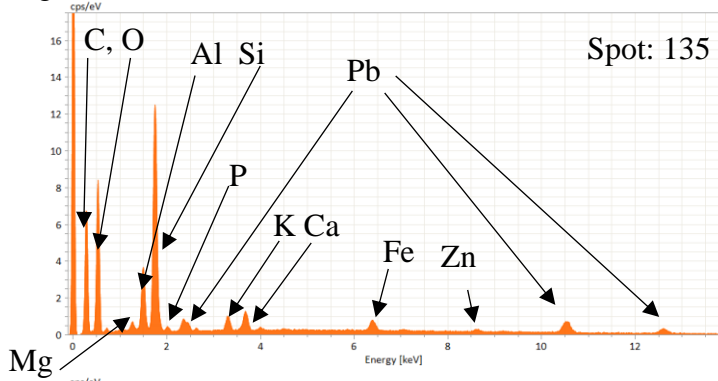
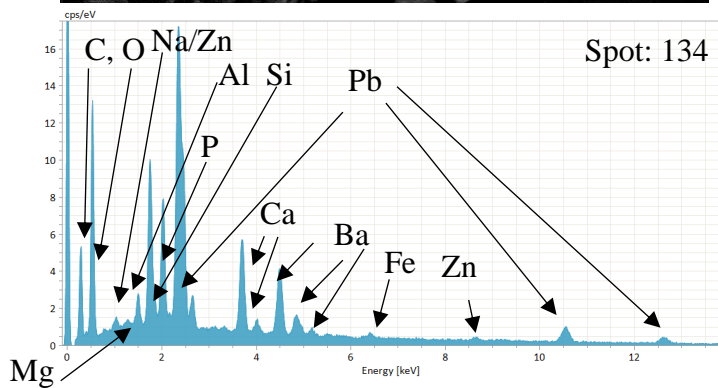
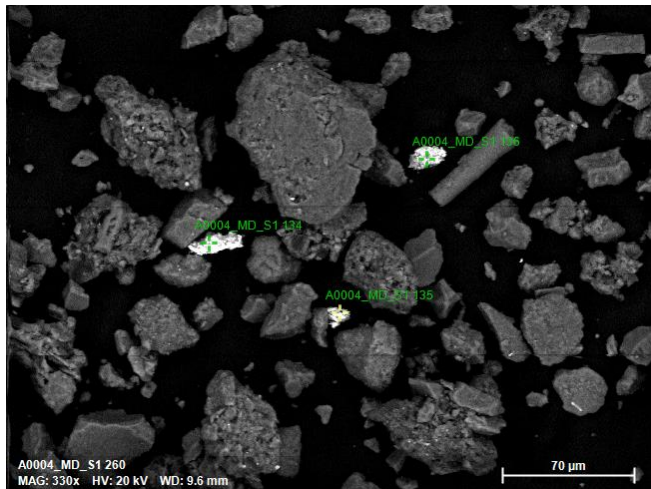


Fig. S19: EDS spot analyses of House 4: Dripline¹⁴. Spot 134 appears likely to be Pb-dominated paint, while Spots 135 and 136 contain much less of an initial Pb peak, indicative of possible X-ray shadowing due to an uneven spot surface. The general compositional similarity between the particles is indicative of Pb paint with slightly different elemental composition, possibly from different paint layers.

555

556

557

558

559

560

561

562

563

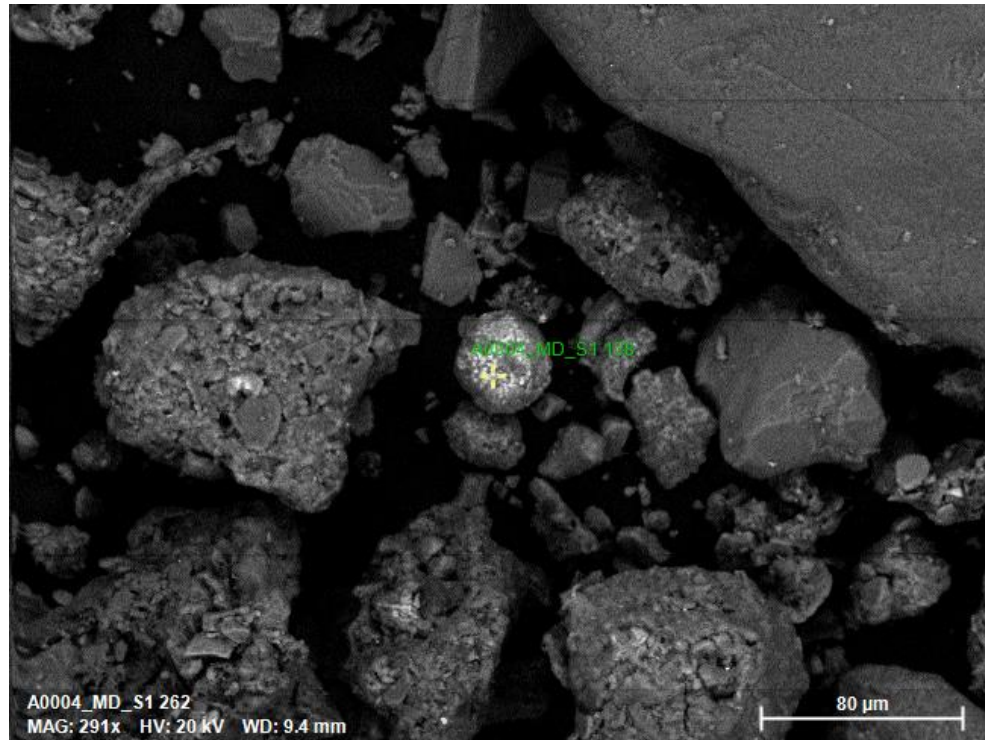
564

565

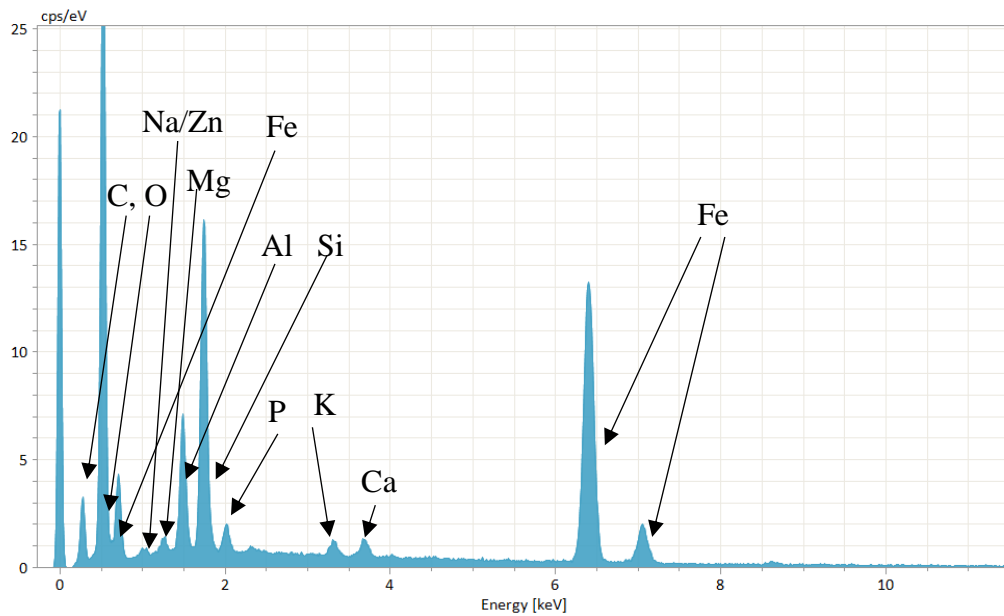
566

567

568



569



570

571

572

573

574

575

576

577

578

579

580 **Fig. S20:** EDS spot analysis of House 4: Dripline¹⁵.

581

582

583

584

585

586

587

588

589

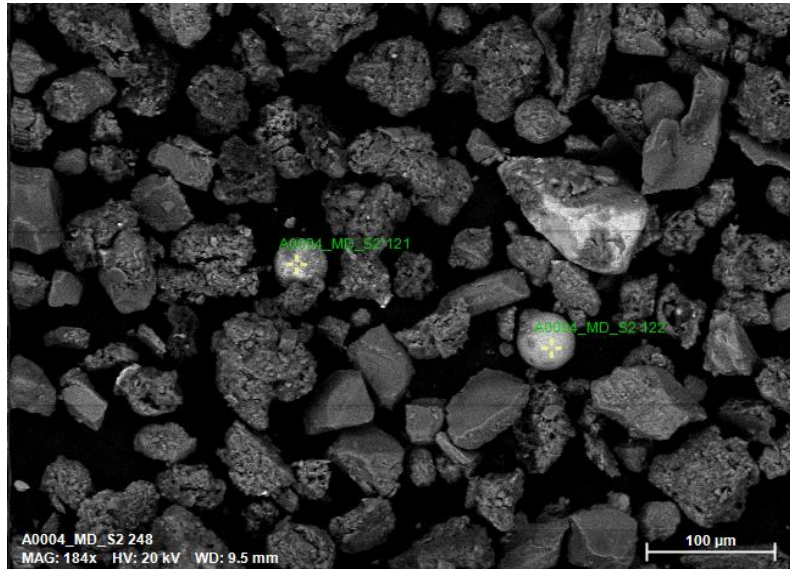
590

591

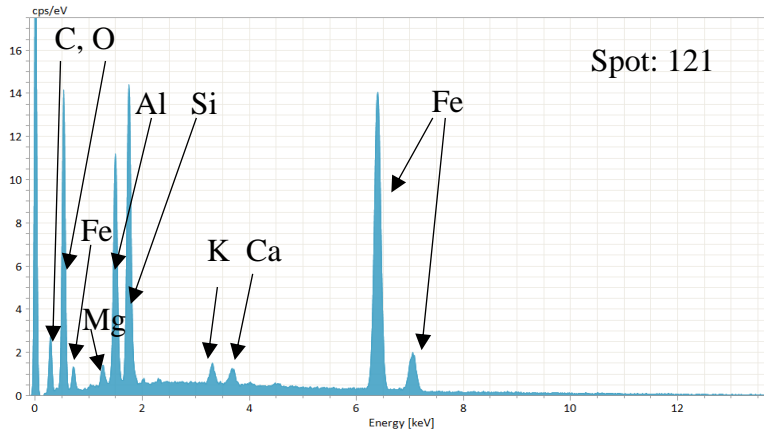
592

593

594



595



596

597

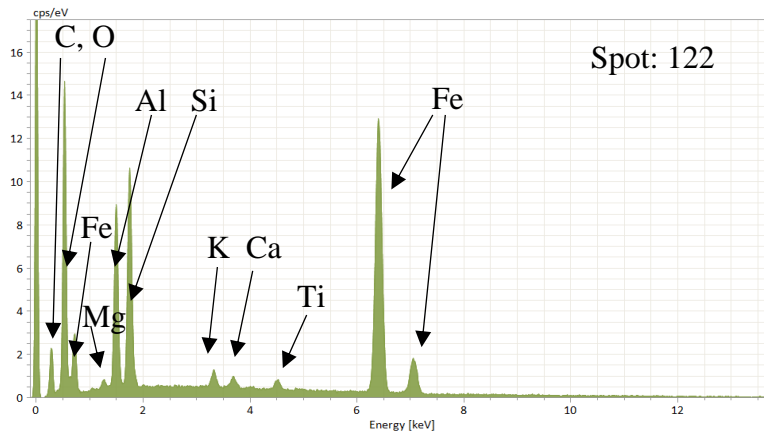
598

599

600

601

602



603

604

605

606

607

608

609

610 **Fig. S21:** EDS spot analyses of House 4: Streetside¹⁶.

611

Supplementary Tables

612 **Table S1:** Bulk metal concentrations (mg/kg) and % recovery relative to certified values for five
 613 subsamples of NIST SRM 2702 – Inorganics in Marine Sediment.

	Cd	Sb	Tl	Pb
Limits of Detection (LOD) (ppb)	0.02	0.03	0.004	0.02
NIST_2702_1	0.67	5.42	0.73	126.20
NIST_2702_2	0.71	5.08	0.76	130.76
NIST_2702_3	0.64	6.23	0.75	127.61
NIST_2702_4	0.66	6.70	0.80	113.82
NIST_2702_5	0.61	6.26	0.77	95.27
Certified Values (mg/kg)	0.817	5.6	0.8267	132.8
% Recoveries	81.51	96.74	87.82	95.03
	87.25	90.64	92.12	98.47
	78.05	111.34	91.06	96.09
	80.78	119.57	96.87	85.71
	74.16	111.73	92.86	71.74
Avg % Recovery	80.35	106.00	92.14	89.41
Std Dev % Recovery	4.82	11.91	3.27	11.00

614

615 **Table S2:** Pb isotopic ratios for NIST SRM 2702 following sample prep that was the same as
 616 soil/dust samples, and Pb isotopic ratios for AGV-2a following standard clean lab protocol, with
 617 the given USGS values. 2σ overall analytical error for all analyses is also provided (based on the
 618 reproducibility of NIST SRM 981 over the course of the analytical session).

619

Reference Standard		208/206	207/206	208/207	206/204	207/204	208/204
	981 2σ external error	0.0001	0.0000	0.0001	0.0014	0.0014	0.0044
	external error (%)	0.005%	0.002%	0.003%	0.008%	0.009%	0.012%
NIST_2702_1		2.05574	0.83455	2.46329	18.77388	15.66794	38.59431
NIST_2702_2		2.05504	0.83421	2.46344	18.78221	15.66851	38.59835
NIST_2702_3		2.05595	0.83479	2.46282	18.76686	15.66631	38.58354
NIST_2702_4		2.05620	0.83479	2.46314	18.76782	15.66712	38.59037
NIST_2702_5		2.05561	0.83441	2.46355	18.77909	15.66944	38.60262
NIST_2702	Std dev	0.00044	0.00025	0.00029	0.00675	0.00121	0.00734

AGV-2a	2.04293	0.82777	2.46799	18.86955	15.61955	38.54962
AGV-2a USGS values				18.864	15.609	38.511
2 σ external error				0.007	0.006	0.020
<i>AGV-2a published range</i>	<i>2.0413 - 2.049</i>	<i>0.8271 - 0.8295</i>		<i>18.851 - 18.889</i>	<i>15.609 - 15.639</i>	<i>38.511 - 38.7127</i>

620

621 **Table S3:** Bulk metal concentrations for soil and dust samples in mg/kg, as well as assigned
622 house number and sample location.

Sample	Cd	Sb	Tl	Pb	House	Sample Location
A0001_MD_D1	1.09	37.60	0.05	104.14	House 1	Dust
A0001_MD_S1	1.32	1.04	0.71	73.05	House 1	Dripline
A0001_MD_S2	1.21	1.50	0.39	103.77	House 1	Street
A0001_MD_S3	1.25	2.42	0.65	127.69	House 1	Yard
A0002_MD_D1	1.12	2.92	0.19	242.47	House 2	Dust
A0002_MD_S1	0.23	0.04	0.03	4.10	House 2	Dripline
A0002_MD_S2	2.09	2.48	0.39	1823.68	House 2	Street
A0002_MD_S3	4.89	3.59	1.03	2098.49	House 2	Yard
A0003_MD_D1	0.61	5.05	0.15	77.61	House 3	Dust
A0003_MD_S1	0.45	0.78	0.21	96.41	House 3	Dripline
A0003_MD_S2	0.92	1.59	0.47	332.93	House 3	Street
A0003_MD_S3	0.90	1.81	0.60	223.74	House 3	Yard
A0004_MD_D1	3.34	1.74	0.25	878.37	House 4	Dust
A0004_MD_S1	2.83	5.17	0.59	1152.48	House 4	Dripline
A0004_MD_S2	1.40	1.30	0.64	347.80	House 4	Street
A0004_MD_S3	0.37	0.90	0.45	70.33	House 4	Yard

623

624 **Table S4:** Pb isotope ratios for soil and dust samples.

Samples	208/206	207/206	208/207	206/204	207/204	208/204
A0001_MD_D1	2.081	0.845	2.463	18.510	15.640	38.521
A0001_MD_S1	2.033	0.826	2.462	18.963	15.659	38.558
A0001_MD_S2	2.010	0.810	2.483	19.404	15.708	39.011
A0001_MD_S3	2.012	0.811	2.480	19.360	15.702	38.944
A0002_MD_D1	2.008	0.808	2.486	19.453	15.714	39.063
A0002_MD_S1	2.001	0.807	2.479	19.458	15.706	38.934
A0002_MD_S2	2.012	0.810	2.483	19.387	15.710	39.006
A0002_MD_S3	2.010	0.808	2.487	19.453	15.719	39.096
A0003_MD_D1	2.065	0.841	2.456	18.599	15.639	38.402
A0003_MD_S1	2.061	0.836	2.465	18.710	15.638	38.554

A0003_MD_S2	2.095	0.865	2.421	18.019	15.592	37.741
A0003_MD_S3	2.054	0.832	2.469	18.812	15.648	38.636
A0004_MD_D1	2.033	0.818	2.486	19.190	15.692	39.017
A0004_MD_S1	2.004	0.802	2.500	19.615	15.727	39.310
A0004_MD_S2	2.019	0.815	2.477	19.261	15.696	38.882
A0004_MD_S3	2.017	0.812	2.483	19.320	15.696	38.976

625

626 **Table S5:** Relative distance between the adjacent main road and front of the household property
627 to the nearest meter, determined via the Google Maps “Measure distance” tool, oldest annual
628 average daily traffic (AADT) data available for the closest major street to the household from the
629 Indiana Department of Transportation* (oldest available data was used to try and match
630 historical traffic flow when leaded gasoline was prominent, although it is noted there is a large
631 disconnect of over 20-30 years from leaded gasoline usage and reported traffic data), and
632 potential industrial sources of pollution with distance determined via the Google Earth
633 measurement tool.

Sample	House	Distance from road to home (meters)	AADT	Potential industrial sources of pollution (distance in km)
A0001_MD	1	14	12,772 ¹	Indianapolis Motor Speedway (2.4 km), lumber facility (1.3 km)
A0002_MD	2	8	2,339 ²	Indiana state fairgrounds (1.8 km), former American Lead facility (2.4 km), fabricated metals facility (1.7 km)

A0003_MD	3	7	21,979 ³	Industrial Park: Oils/solvents, automobile parts, construction company, storage units, pallets (<1 km)
A0004_MD	4	8	2,203 ⁴	Fabricated metals facility (1.7 km), Indianapolis Motor Speedway (3.6 km)

634 ¹W. 30th Street, 2013.

635 ²N. Washington Blvd, 2013.

636 ³S. Harding Street, 2016.

637 ⁴N. Harding St., 2013.

638 *[Traffic Count Database System \(TCDS\) \(ms2soft.com\)](http://ms2soft.com)

639

640

Supplementary References

641 Dietrich, M., Krekeler, M. P., Kousehlar, M., & Widom, E. (2021). Quantification of Pb
642 pollution sources in complex urban environments through a multi-source isotope mixing model
643 based on Pb isotopes in lichens and road sediment. *Environmental Pollution*, 288, 117815.

644 Galer, S. J. G., & Abouchami, W. (1998). Practical application of lead triple spiking for
645 correction of instrumental mass discrimination. *Mineral. Mag. A*, 62, 491-492.

646 Jeong, H., Ra, K., & Choi, J. Y. (2021). Copper, Zinc and Lead Isotopic Delta Values and
647 Isotope Ratios of Various Geological and Biological Reference Materials. *Geostandards and
648 Geoanalytical Research*, 45 (3), 551–563.

649 Kousehlar, M., & Widom, E. (2020). Identifying the sources of air pollution in an urban-
650 industrial setting by lichen biomonitoring-A multi-tracer approach. *Applied Geochemistry*, 121,
651 104695.

- 652 LeGalley, E., Widom, E., Krekeler, M. P., & Kuentz, D. C. (2013). Chemical and lead isotope
653 constraints on sources of metal pollution in street sediment and lichens in southwest
654 Ohio. *Applied Geochemistry*, 32, 195-203.
- 655 Smith, D.B., Cannon, W.F., Woodruff, L.G., Solano, Federico, Kilburn, J.E., and Fey, D.L.,
656 2013, Geochemical and mineralogical data for soils of the conterminous United States: U.S.
657 Geological Survey Data Series 801, 19 p., <https://pubs.usgs.gov/ds/801/>.
- 658 Wang, Z., Dwyer, G. S., Coleman, D. S., & Vengosh, A. (2019). Lead isotopes as a new tracer
659 for detecting coal fly ash in the environment. *Environmental Science & Technology*
660 *Letters*, 6(12), 714-719.